

DESIGN OF OPTIMAL AND SUBOPTIMAL TEMPERATURE  
CONTROL SYSTEMS FOR AN ELECTRIC CLOTHES DRYER

A THESIS

Presented to

The Faculty of the Graduate Division

by

William Hilton Preetz

In Partial Fulfillment

of the Requirements for the Degree

Master of Science in Electrical Engineering

Georgia Institute of Technology

September, 1971

In presenting the dissertation as a partial fulfillment of the requirements for an advanced degree from the Georgia Institute of Technology, I agree that the Library of the Institute shall make it available for inspection and circulation in accordance with its regulations governing materials of this type. I agree that permission to copy from, or to publish from, this dissertation may be granted by the professor under whose direction it was written, or, in his absence, by the Dean of the Graduate Division when such copying or publication is solely for scholarly purposes and does not involve potential financial gain. It is understood that any copying from, or publication of, this dissertation which involves potential financial gain will not be allowed without written permission.

---

0

7/25/68

DESIGN OF OPTIMAL AND SUBOPTIMAL TEMPERATURE  
CONTROL SYSTEMS FOR AN ELECTRICAL CLOTHES DRYER

Approved: \_\_\_\_\_

Chairman / \_\_\_\_\_ / \_\_\_\_\_

Date Approved by Chairman: 8/11/71

To Evelyn and  
Mom

## ACKNOWLEDGMENTS

I would like to express my profound gratitude to my thesis advisors, Dr. James R. Rowland and Dr. Jay H. Schlag, for their constant encouragement and guidance in the preparation of this thesis. Special thanks are also due to Dr. Dale C. Ray and Dr. Roger P. Webb, the members of my reading committee.

I would also like to express my appreciation to the Whirlpool Corporation both for financial support and for technical assistance from the Advanced Development group in St. Joseph, Michigan. In particular, I would like to thank Mr. Jack F. Clearman, Mr. R. Bruce Sherer, Mr. Jerry I. Schornhorst, and Mr. R. Trezevant Wigfall of Whirlpool.

Finally, to my typist, Mrs. Peggy Green, goes an expression of gratitude for her assistance in the preparation of this document.

## TABLE OF CONTENTS

	Page
ACKNOWLEDGMENTS . . . . .	iii
LIST OF TABLES . . . . .	vi
LIST OF ILLUSTRATIONS . . . . .	vii
SUMMARY . . . . .	ix
Chapter	
I. INTRODUCTION . . . . .	1
The Problem	
Dryer Operation	
Literature Review	
Method of Attack	
Thesis Outline	
II. IDENTIFICATION OF THE PLANT . . . . .	13
Introduction	
The Modeling Problem	
Digital Computer Results	
Analog Computer Results	
Summary	
III. OPTIMAL CONTROL STRATEGY . . . . .	27
Introduction	
Phase Plane	
Switching Curve	
Optimal Controller	
Sensitivity Analysis	
Summary	
IV. SUBOPTIMAL CONTROL STRATEGY . . . . .	46
Introduction	
Proportional-plus-derivative Switching Curve	
Proportional-plus-derivative Controller	
Sensitivity Analysis	
Summary	

Table of Contents Continued	Page
V. CONCLUSIONS AND RECOMMENDATIONS . . . . .	54
Conclusions	
Recommendations	
APPENDIX . . . . .	57
BIBLIOGRAPHY . . . . .	62

## LIST OF TABLES

Table		Page
1.	Input Data for the Dryer Simulation Using Permanent Press Material . . . . .	13
2.	Comparison of the Whirlpool Simulation and the Least-Square Method . . . . .	18



## LIST OF ILLUSTRATIONS

Figure		Page
1.	Simplified Diagram of Clothes Dryer . . . . .	3
2.	Mass of Water in Clothes and Drying Rate . . . . .	4
3.	Inlet and Exhaust Temperatures . . . . .	4
4.	Temperature Control System Block Diagram . . . . .	10
5.	Electric Heater Power $Q(t)$ and Corresponding Exhaust Temperature $T_E(t)$ . . . . .	14
6.	Electric Heater Power $Q(t)$ and Corresponding $T(t)$ , the Increase in Exhaust Temperature Over Room Temperature in Falling-Rate Region . . . . .	16
7.	Comparison Between $T(t)$ in Whirlpool Simulation and Least-Squares Curve Fit Model . . . . .	20
8.	Analog Computer Circuit for Plant Identification . . . . .	22
9.	Comparison Between $T(t)$ in Whirlpool Simulation and Analog Simulation of Heating Equation . . . . .	23
10.	Comparison Between $T(t)$ in Whirlpool Simulation and Analog Simulation of Cooling Equation . . . . .	24
11.	System Block Diagram with Mathematical Model of Plant . . . . .	26
12.	Analog Computer Circuit for Phase Plane Plots . . . . .	28
13.	Phase Plane for Heating and Cooling Equations . . . . .	29
14.	Optimal Control System Block Diagram . . . . .	38
15.	Deviations in Phase Plane Trajectories Resulting from Parameter Variations . . . . .	43

## List of Illustrations Continued

Figure	Page
16. Proportional-Plus-Derivative Switching Curve with Hysteresis . . . . .	48
17. Suboptimal Proportional-Plus-Derivative Control System Block Diagram . . . . .	50

## SUMMARY

Recently, synthetic fabrics have been discovered which are easily destroyed under the influence of excessive temperature. Accordingly, Whirlpool Corporation sponsored this research in the hopes of discovering an improved temperature control system for electric clothes dryers. The specific objective is to develop a controller which increases the exhaust temperature from room temperature to  $150^{\circ}$  F in minimum time. It is subsequently desired to maintain that temperature within  $\pm 1^{\circ}$  F until the clothes are dry. The method of attack involves the development of a mathematical model for a set of nominal operating conditions. Both an optimal controller and a more practical suboptimal controller are then designed on the basis of this model.

The mathematical model consists of two linear second-order differential equations, one of which is valid while the heater is on, the other, while the heater is off. The model is derived empirically using numerical analysis techniques on a digital computer. It is most accurate for the following operating conditions: eight pounds of permanent press material with  $70^{\circ}$  F room temperature and 50 per cent relative humidity.

The optimal controller is determined through the use of phase plane analysis. The complex optimal switching equation is derived by modern control theory techniques. Sensitivity studies indicate good results when parameters are varied. However, the optimal controller is both complex and physically unrealizable.

A suboptimal controller is developed to overcome these objections. This system attains an exhaust temperature of  $150^{\circ}\text{ F} \pm 1^{\circ}\text{ F}$  in minimum time and subsequently maintains this tolerance for the preceding nominal conditions. System performance deteriorates when certain parameters are varied. However, the suboptimal controller designed herein provides better temperature control than than the current production proportional control system.

## CHAPTER I

### INTRODUCTION

#### The Problem

Clothing manufacturers will soon commence production of a new generation of synthetic fabrics, which will be quite sensitive to excessive temperature. There is a definite possibility that some of these fabrics will be destroyed by the temperature control system in present-day dryers. On production dryers today, there is a thermostatic proportional control system which suffers from excessive temperature overshoots and undershoots as well as from a large thermostatic temperature differential. Thus, after initially reaching  $150^{\circ}$  F, the present dryer exhaust temperature can overshoot to  $155^{\circ}$  F, be subjected to thermostat hysteresis and undershoot to  $130^{\circ}$  F. Since minimum drying time requires rapid acceleration to a high temperature and subsequent maintenance of that high temperature, it would be inefficient to prevent fabric damage by simply lowering the thermostat cycle temperature. A safe yet efficient control scheme would be to translate the exhaust temperature to  $150^{\circ}$  F in minimum time and maintain  $\pm 1^{\circ}$  F thereafter. To this end, both an optimal and a suboptimal control system are advanced.

The strategy is to develop a mathematical model of the heating-cooling system of the clothes dryer and then to simulate this model on



a digital computer. The developed model has electrical power into the heater as the plant input and the difference between exhaust temperature and room temperature as the plant output. A linear second-order differential equation represents the transfer function relating the input and output. This model is verified with data from an existing Whirlpool dryer computer simulation. Both an optimum control strategy and a proportional-plus-derivative suboptimum control strategy are developed on the basis of this plant model.

### Dryer Operation

In current production clothes dryers, a fan in the exhaust duct draws air at ambient temperature through an inlet duct and across an electric heater as shown in Figure 1. This heated air then flows into a rotating drum which contains the clothes load. Heat is transferred to the clothes while moisture is transferred to the air. The cooler but more humid air is then exhausted to the atmosphere. The exhaust temperature is monitored with a bimetallic thermostat which controls the heater.

The drying process itself can be divided into three distinct phases. They are the warm-up phase, steady-state phase, and falling-rate phase as shown in Figures 2 and 3. In the warm-up phase, power is initially applied to the heater resulting in an exponential rise in the effective drum inlet temperature  $T_I(t)$  to a steady-state value. Meanwhile, the drying rate  $\dot{M}_w(t)$  and the exhaust temperature  $T_E(t)$  are also rising exponentially to steady-state values. The duration of the warm-up phase is on the order of five minutes.

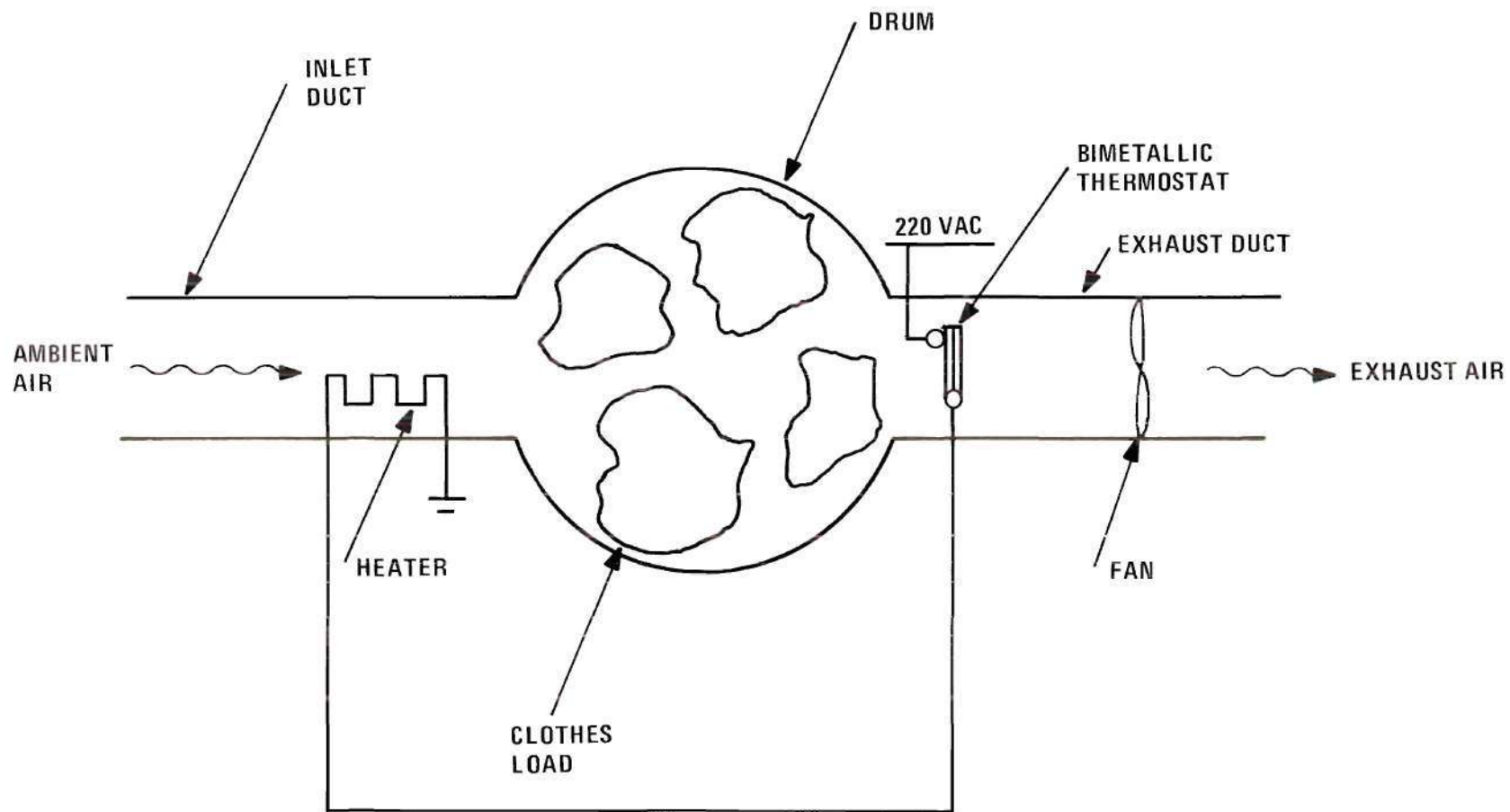


Figure 1. Simplified Diagram of Clothes Dryer.

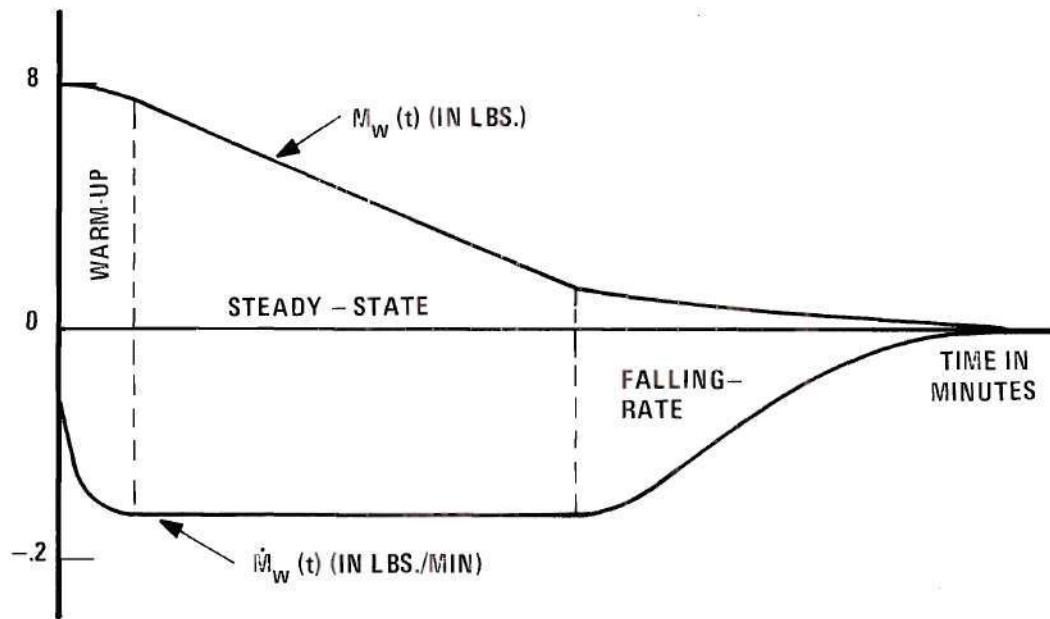


Figure 2. Mass of Water in Clothes and Drying Rate.

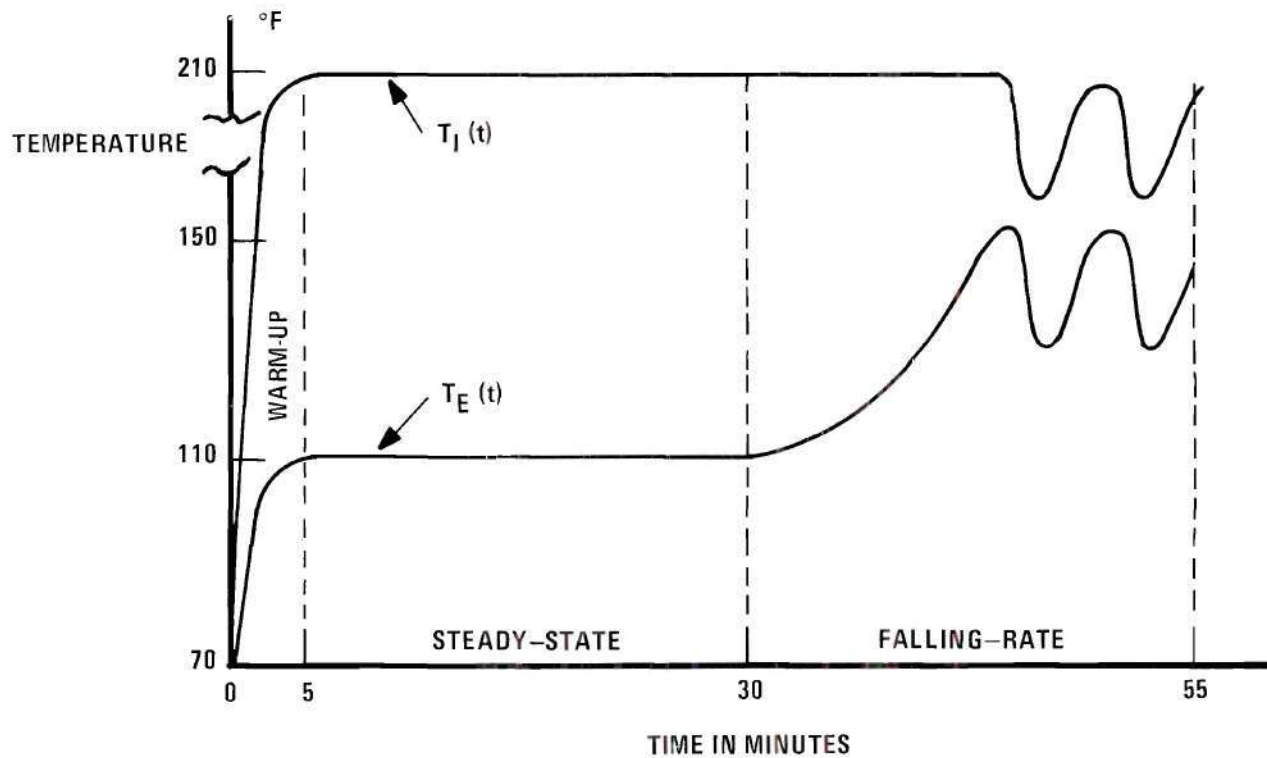


Figure 3. Inlet and Exhaust Temperatures.



In the steady-state phase, the drying rate and the inlet and exhaust temperatures remain constant with respect to time. The duration of this phase is typically five or six times greater than the warm-up phase.

The falling rate region is the least understood of the three regions. This phase commences when there are no longer continuous threads of moisture in the clothes. The breakdown of continuous moisture threads sharply reduces the mobility of the water. As a result, the migration of moisture in the falling rate region is accomplished entirely by the evaporation-condensation mechanism. This results in a gradually decreasing drying rate while the exhaust temperature increases substantially. The initial falling-rate temperature is typically  $100^{\circ}\text{F}$  to  $130^{\circ}\text{F}$  whereas the final temperature would approach the vicinity of  $200^{\circ}\text{F}$  if no feedback control were provided. In present production machines the exhaust temperature will typically cycle up to four times from  $130^{\circ}\text{F}$  to  $155^{\circ}\text{F}$ . As previously noted, this performance is now deemed unacceptable.

#### Literature Review

The desirability of an improved heater control system is demonstrated by Hurley [1]. He shows that fabric shrinkage, or even fabric destruction, are problems resulting from excessive temperature cycling as well as excessive temperatures. In the case of acrylic knitted fabrics, Hurley finds that every  $4.2^{\circ}\text{F}$  of thermostatic temperature differential increases area shrinkage by 1 per cent. The present  $15^{\circ}\text{F}$  differential alone could account for nearly 4 per cent

area shrinkage of an acrylic knitted fabric. Fanson and Tibbitts [2] develop the clothes dryer heat and mass transfer relationships for the warm-up and the steady-state regions of operation. They take advantage of both theoretical and empirical methods in achieving results. Unfortunately, most of their relationships are not valid in the third and final region of operation, i. e. the falling-rate region. This is indeed unfortunate because only in the falling-rate region is the temperature control problem critical. Tibbitts [3] also develops a mass and heat energy balance equation. While this equation is quite accurate throughout the drying cycle, it is a function of many variables. Hughes [4] finds a functional relationship between the mass of water in the clothes and time. This equation is also valid in the falling-rate region. He recommends the use of simplified rather than overly complex models when dealing with the falling-rate region. Hughes [5] also states that the dynamics of the falling-rate region are a function of material, load weight, and ambient conditions in a given machine. He suggests the use of empirical methods in dealing with this phase of operation.

The suboptimum control strategy for heater control in this thesis is based on the work of Knoop and Becker [6], who develop the theory for an electronic heater control system for an electric range. They derive a second-order linear mathematical model for the heat transfer process neglecting mass transfer and then design a "bang-zero, proportional-plus-derivative" controller. The authors [7] also design actual hardware for a suboptimum range control. The solid-state circuitry features a thermistor in a bridge configuration for determining the error signal, a differentiator, a summing amplifier, a comparator and a triac for

power switching.

Melsa and Schultz [8], for example, discuss the complete second order step response. They also show the effect of variation of the parameters damping  $\delta$ , natural frequency  $\omega_n$ , and gain  $K$ . The decision to derive an empirical model leads to the consideration of a least-squares curve fit [9]. Heater control strategies, including the use of secondary feedback elements, are discussed extensively by Roots and Walker [10-11]. Hanchett [12] designs a number of heater control circuits. It should be pointed out that these three papers consider temperature controls in buildings rather than dryer temperature controls. However, they do discuss the use of thermostats quite extensively. The basic form of control strategy selected for the problem at hand can be found in Hsu and Meyer [13]. It consists of plotting state variable trajectories on a state plane and solving for the optimum switching function.

#### Method of Attack

The basic approach involves both the mathematical simulation of a convective clothes dryer and the development of optimal and suboptimal control strategies to control the exhaust temperature. It should be noted that the desired temperature of  $150^{\circ}\text{F}$  is invariably first attained in the falling-rate region and not in the steady-state or warm-up region. As a result of this observation, it is only necessary to develop the mathematical model for the falling-rate region of operation.

#### Simulation of the Dryer

The exhaust temperature is simulated as a function of heater power



and elapsed time in the falling rate region. A mathematical model is derived empirically by use of numerical analysis techniques. Data for the simulation is obtained from a Whirlpool Corporation dryer simulation computer program. The Whirlpool program provides the exhaust temperature as a function of both elapsed time and heater power for various ambient conditions. A second-order differential equation is developed to simulate the exhaust temperature for a nominal clothes load, i. e. eight pounds of permanent press material containing six pounds of water at 90° F, and nominal ambient conditions, i. e. 70° F room temperature and 50 per cent relative humidity. The equation is of the basic form

$$\ddot{T}(t) + c_1 \dot{T}(t) + c_0 T(t) = b_0 Q(t)$$

where  $T(t)$  is the difference between the exhaust temperature and room temperature,  $Q(t)$  is the heater power, and  $c_0$ ,  $c_1$  and  $b_0$  are constants determined by a least-squares curve fit computer program. The derivatives at the various data points are approximated by appropriate finite difference equations. Thus, at each data point, the exhaust temperature, the first and second derivatives of temperature, and the heater input power are known quantities. The three unknown constant coefficients,  $c_0$ ,  $c_1$  and  $b_0$  are then determined by a least-squares method.

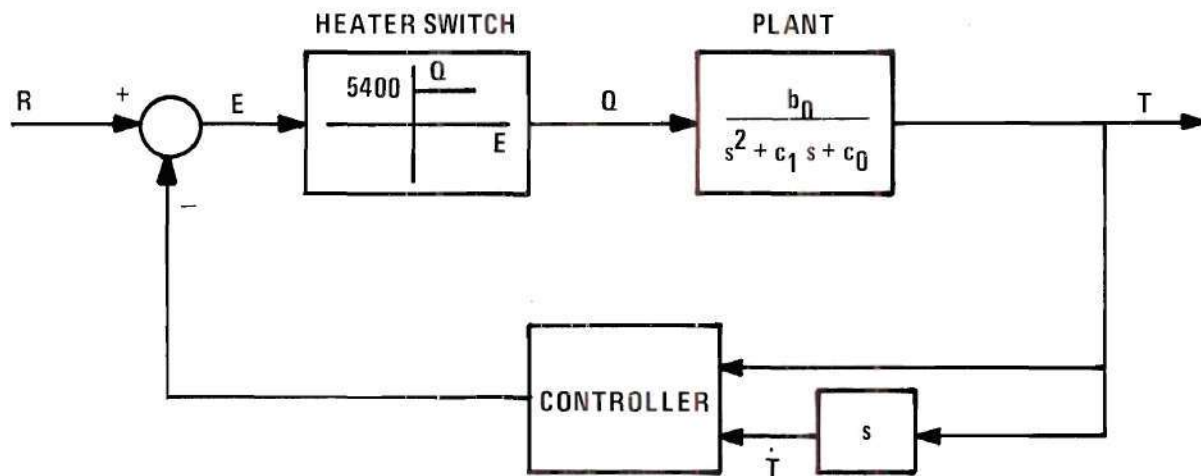
As previously stated, the thermodynamics of the falling rate region are quite complex. The exhaust temperature is actually a function of material, load weight and ambient conditions. This implies that  $c_0$ ,  $c_1$  and  $b_0$  are also functions of these variables. However, for the preceding clothes load and operating conditions, which were chosen as being average

or representative of situations encountered in normal use of the machine,  $c_0$ ,  $c_1$  and  $b_0$  would be constants. While the above model may not be highly accurate for pathological cases, i. e. operating conditions or clothes load far different than the above nominal, it is expected to be sufficiently accurate for conditions in the vicinity of the preceding nominal set. A sensitivity analysis is conducted to confirm this hypothesis.

#### Optimum and Suboptimum Control Strategies

A proportional-plus-derivative suboptimal control system as well as the optimal control system is developed after the equation of the plant has been determined. In both cases, the control variable is the difference between the exhaust temperature and room temperature. A complete system block diagram is illustrated in Figure 4. The system can be categorized as a dual-mode control system because the heater is constrained to operate either full-on or full-off. Since the equation of the plant is second-order, phase plane analysis techniques can be utilized. It is then a straight-forward problem to determine the equation of the optimal switching curve.

Physically realizable controllers are developed to approximate the optimal control system mentioned above. These results are utilized with the optimal switching curve to design a suboptimal solution which is relatively insensitive to errors in switching conditions and system parameters. Upon reaching the desired exhaust temperature of  $150^{\circ}$  F, the optimal controller switches the heater on and off at theoretically infinite frequency while the exhaust temperature remains at  $150^{\circ}$  F. This is a problem referred to in the literature as relay chatter.



R – Reference Temperature

E – Error Signal

Q – Electric Power of Heater

$c_0, c_1, b_0$  – Constants Determined by Least-Squares Method

s – Laplace Transform Operator

T – Difference Between Exhaust Temperature and Assumed Room Temperature of 70° F

$\dot{T}$  – Time Derivative of T

Figure 4. Temperature Control System Block Diagram.

Another disadvantage of optimal control lies in its complexity. Accordingly, a simpler, suboptimal proportional-plus-derivative controller is also designed. This controller eliminates relay chatter by feeding back the heater signal, thus translating the switching curve back and forth every half (switching) cycle. This results in a limit cycle with the exhaust temperature varying between the prescribed limits of  $149^{\circ}\text{ F}$  and  $151^{\circ}\text{ F}$ .

### Thesis Outline

Following this introductory chapter, the identification of the heating-cooling system is presented in Chapter II. An attempt is made to model the entire heating-cooling operation by a single second-order differential equation. Using data from the Whirlpool dryer simulation program, a least-squares curve fit is obtained on the digital computer. This result is subsequently refined by modeling the heating and cooling operations separately. Analog computer curves indicate very accurate results are obtained by using this second approach.

Chapter III describes the design of the optimal controller. Analytical expressions are derived for the optimal switching curve before the optimal controller is presented. Finally, a parameter sensitivity analysis is conducted.

After defining the optimal solution to the given problem, a more practical suboptimal solution is proposed in Chapter IV. The suboptimal controller is a slightly modified form of proportional-plus-derivative control. It is shown that this solution is relatively insensitive to variations in system conditions.

Chapter V contains conclusions and recommendations for further work.



## CHAPTER II

## IDENTIFICATION OF THE PLANT

Introduction

In Chapter I, it is observed that the reference temperature of  $150^{\circ}$  F is invariably attained for the first time in the falling-rate region of operation. Consequently, only the falling-rate region is modeled. Data for the identification problem is obtained from a Whirlpool Corporation dryer simulation computer program. This program provides the exhaust temperature versus time and heater power as shown in Figure 5 for the nominal ambient conditions of Table 1.

Table 1. Input Data for the Dryer Simulation  
Using Permanent Press Material

---

Ambient dry bulb = $70^{\circ}$ F
Relative Humidity = 50 per cent
Clothes Load Weight = 8 pounds
Initial Load Temperature = $90^{\circ}$ F
Initial Load Moisture Content = 75 per cent
Air Flow = 120 CFM
Main Heater Wattage = 5400
Secondary Heater Wattage = 0

---

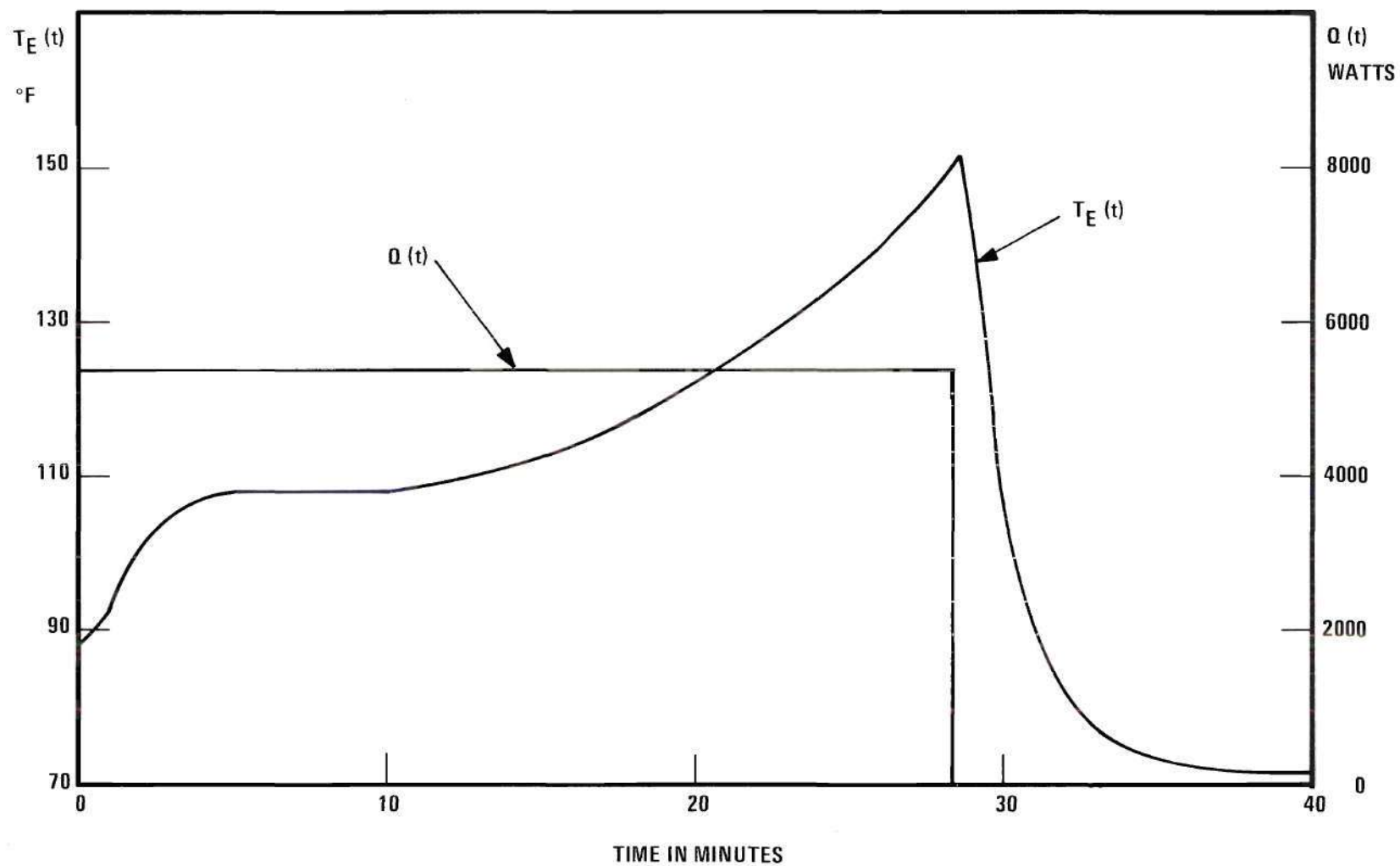


Figure 5. Electric Heater Power  $Q(t)$  and Corresponding Exhaust Temperature  $T_E(t)$ .

Figure 6 illustrates  $T(t)$ , the difference between exhaust temperature and room temperature in the falling rate region.  $T(t)$  is defined by

$$T(t) = T_E(t) - 70^{\circ} \text{ F} \quad (2.1)$$

where  $70^{\circ} \text{ F}$  is the assumed room temperature. The relationship of the two curves suggests that  $T(t)$  could be approximated as a second-order step response to an input  $Q(t)$  with an initial condition  $T(0) = 37.5^{\circ} \text{ F}$ . The derivation of this second order transfer function is the goal of Chapter II.

### The Modeling Problem

The objective is to find the coefficients  $a_0$ ,  $a_1$  and  $b$  of the second-order differential equation

$$a_0 \ddot{T}(t) + a_1 \dot{T}(t) + T(t) = b Q(t) \quad (2.2)$$

such that the solution  $T(t)$  is related to the exhaust temperature  $T_E(t)$  in the falling-rate region. This problem can be solved by a number of frequency domain methods, such as the method of moments, the z-transform method, and Guillemin's Fourier Series method [14]. However, these methods can result in additional errors in the frequency domain, such as the required use of Pade approximations to time delays. These methods can also result in an unstable model to represent a stable system, which is an undesirable characteristic. Accordingly, a time domain approach is utilized in this thesis. Such a time-domain method which minimizes the least-square error is presented in the appendix.

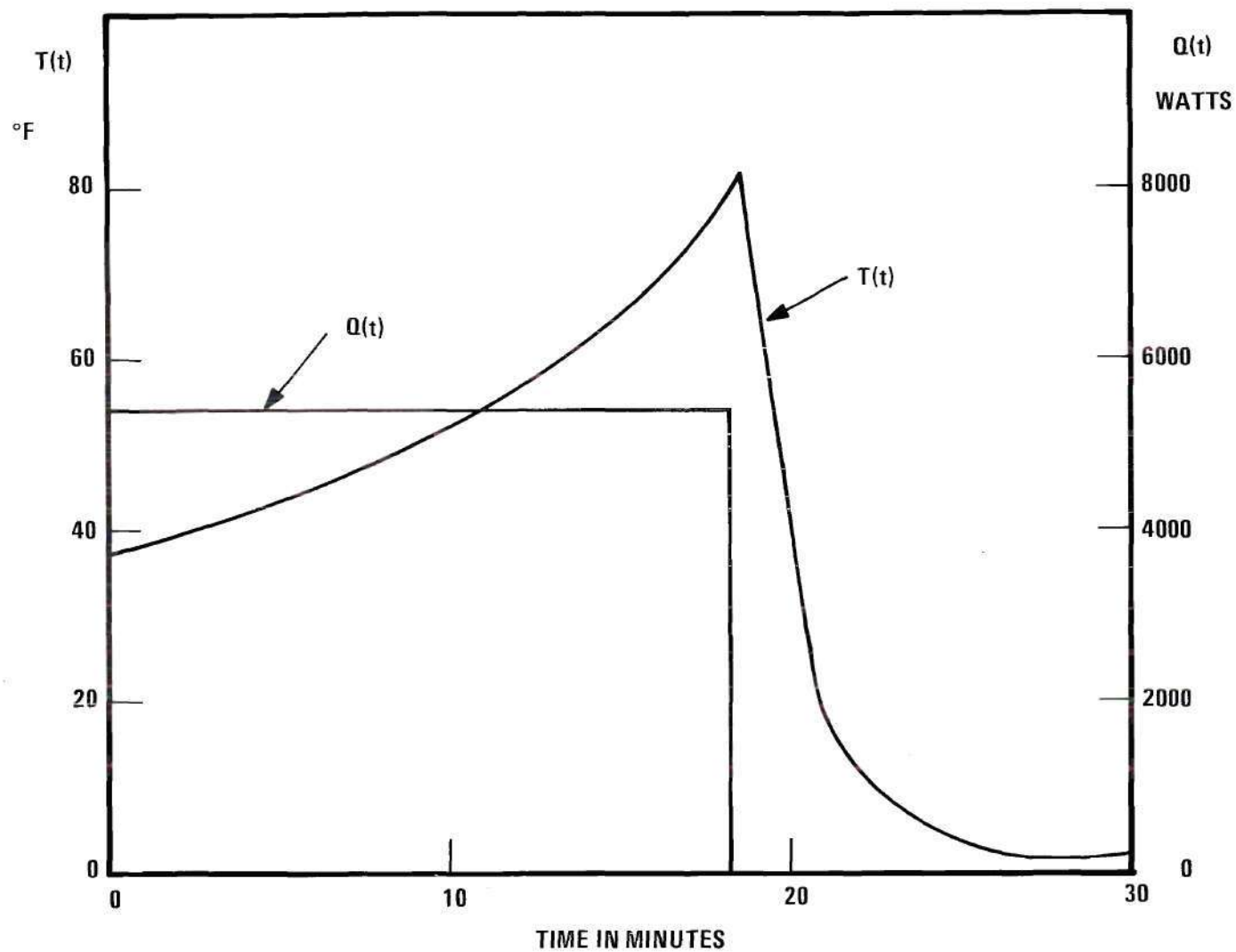


Figure 6. Electric Heater Power  $Q(t)$  and Corresponding  $T(t)$ , the Increase in Exhaust Temperature Over Room Temperature in Falling-Rate Region.

### Digital Computer Results

Equation (A.11) in the appendix can be readily solved for  $a_0$ ,  $a_1$  and  $b$  on a digital computer. A program which accomplishes this has been written in GTL (Georgia Tech Language--an extended version of Algol) and executed on a Burrough B5500 computer. The digital program predicts the following second-order differential equation for falling-rate operation:

$$\ddot{T}(t) + 1.82319 \dot{T}(t) + 0.98287 T(t) = 0.01064 Q(t) \quad (2.3)$$

The Whirlpool simulation values for temperature in the falling rate region and the solution to (2.3) are tabulated in Table 2 and plotted in Figure 7. It is apparent that the least-squares method fails to yield a satisfactory second-order differential equation in the region of interest. There are two basic reasons for this result. First, the matrix of (A.10) is ill-conditioned.

$$= \begin{bmatrix} \sum \ddot{T}_n^2 & \sum \dot{T}_n \ddot{T}_n & -\sum Q_n \ddot{T}_n \\ \sum \ddot{T}_n \dot{T}_n & \sum \dot{T}_n^2 & -\sum Q_n \dot{T}_n \\ -\sum \ddot{T}_n Q_n & -\sum \dot{T}_n Q_n & \sum Q_n^2 \end{bmatrix}$$

$$= \begin{bmatrix} 1969.65814 & 4.61277 & 8722.22219 \\ 4.61277 & 1876.89532 & -2.48050 \times 10^5 \\ 8722.22219 & -2.48050 \times 10^5 & 5.54040 \times 10^8 \end{bmatrix} \quad (2.4)$$

Equation (2.4) is ill-conditioned because the elements differ from each other by several orders of magnitude. A very small error in one of the elements of (2.4) causes a large error in the resulting inverse matrix

Table 2. Comparison of the Whirlpool Simulation  
and the Least-Square Method

Time (Minutes)	Heater Power (Watts)	Whirlpool Simulation Falling Rate Temperature (°F)	Least-Squares Falling Rate Temperature (°F)
0.0	5400	37.5	37.5
0.9	5400	38.0	42.4
1.8	5400	39.0	49.2
2.7	5400	40.1	54.0
3.6	5400	41.2	56.6
4.5	5400	42.5	57.7
5.4	5400	43.8	58.2
6.3	5400	45.2	58.4
7.2	5400	46.6	58.5
8.1	5400	48.2	58.5
9.0	5400	49.9	58.5
9.9	5400	51.7	58.5
10.8	5400	53.7	58.5
11.7	5400	55.8	58.5
12.6	5400	58.1	58.5
13.5	5400	60.6	58.5
14.4	5400	63.3	58.5
15.3	5400	66.4	58.5
16.2	5400	69.8	58.5
17.1	5400	73.6	58.5
18.0	5400	78.0	58.5



Table 2 Continued

Time (Minutes)	Heater Power (Watts)	Whirlpool Simulation Falling Rate Temperature (°F)	Least-Squares Falling Rate Temperature (°F)
18.9	0	76.0	44.9
19.8	0	46.9	25.8
20.7	0	26.1	12.6
21.6	0	14.3	5.4
22.5	0	8.1	2.0

of (A.11). It is observed that the addition of  $10^{-3}$  to each of the diagonal elements of (2.4) results in some of the inverse matrix elements actually doubling their values. Thus, a small error in one of the elements of the matrix in (A.10) could result in a 50 per cent error in the values of  $a_0$ ,  $a_1$  and  $b$  in (A.11). Second, the total falling-rate response is in all likelihood not exactly second-order with two poles and no zeros.

The least-squares method and the digital computer are now abandoned in favor of a new approach. The result of (2.3), however, is utilized in the new approach which involves an analog computer.

#### Analog Computer Results

Equation (2.3) is simulated on an analog computer with the time scale speeded up so that one minute of real time equals one second of computer time. Magnitude scaling consists of letting one degree Fahrenheit equal 100 millivolts and one watt equal 10 millivolts. The

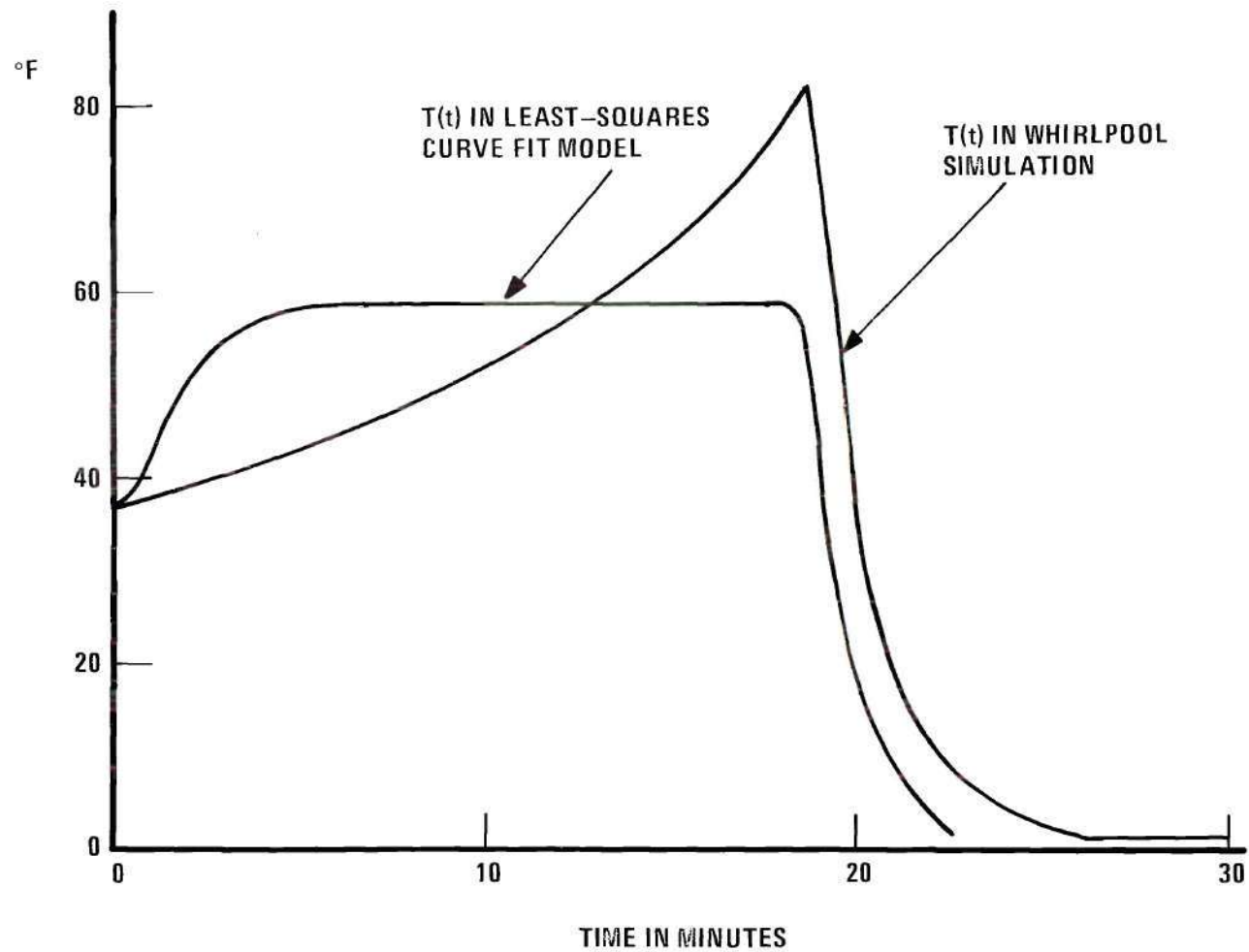


Figure 7. Comparison Between  $T(t)$  in Whirlpool Simulation and Least-Squares Curve Fit Model.



analog circuit is shown in Figure 8.

The objective of the analog simulation is to vary the coefficients of (2.3) such that its solution more closely matches the Whirlpool simulation data of Table 2 and Figure 7. Setting potentiometers P1 to zero and P2 to .03 results in the much improved curve fit of Figure 9. This corresponds to the real-time equation

$$\ddot{T}(t) + 0.03 \dot{T}(t) = 4.74 \times 10^{-5} Q(t) \quad (2.5)$$

with

$$T(0) = 37.5$$

$$\dot{T}(0) = 0$$

Equation (2.5), however, is only valid as a heating curve. If the heater power  $Q(t)$  is turned off, (2.5) does not agree with the true cooling response.

Setting potentiometers P1 to .1, P2 to .22 and P3 to zero yields the curve of Figure 10. This is the solution of the real-time equation

$$\ddot{T}(t) + 2.2 \dot{T}(t) + T(t) = 0 \quad (2.6)$$

with

$$T(18.7) = 80.2$$

$$\dot{T}(18.7) = 0$$

Equation (2.6), which is quite similar to the digital computer's predicted equation (2.3), is classified as a cooling curve. The results to this

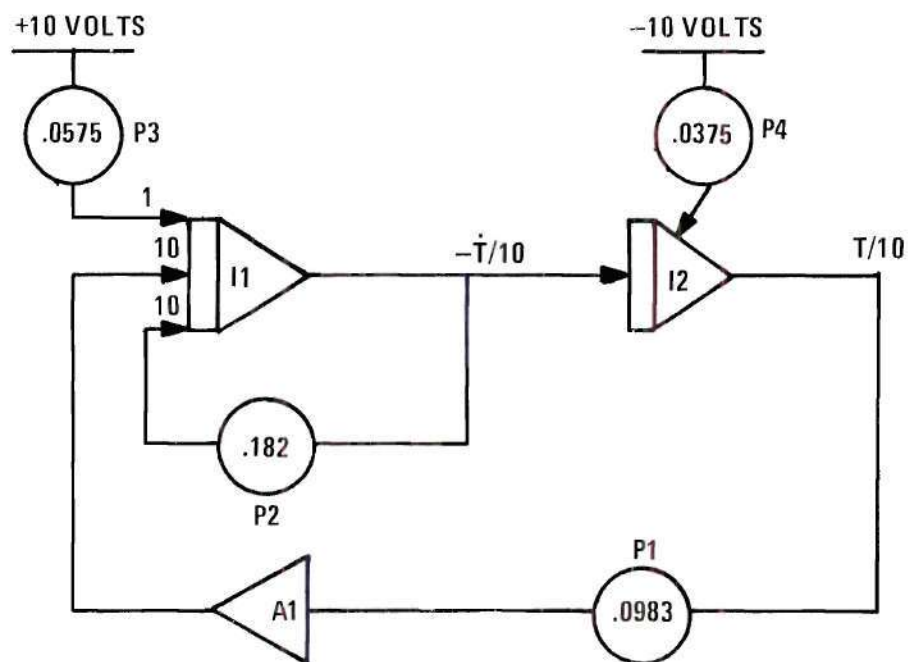


Figure 8. Analog Computer Circuit for Plant Identification.

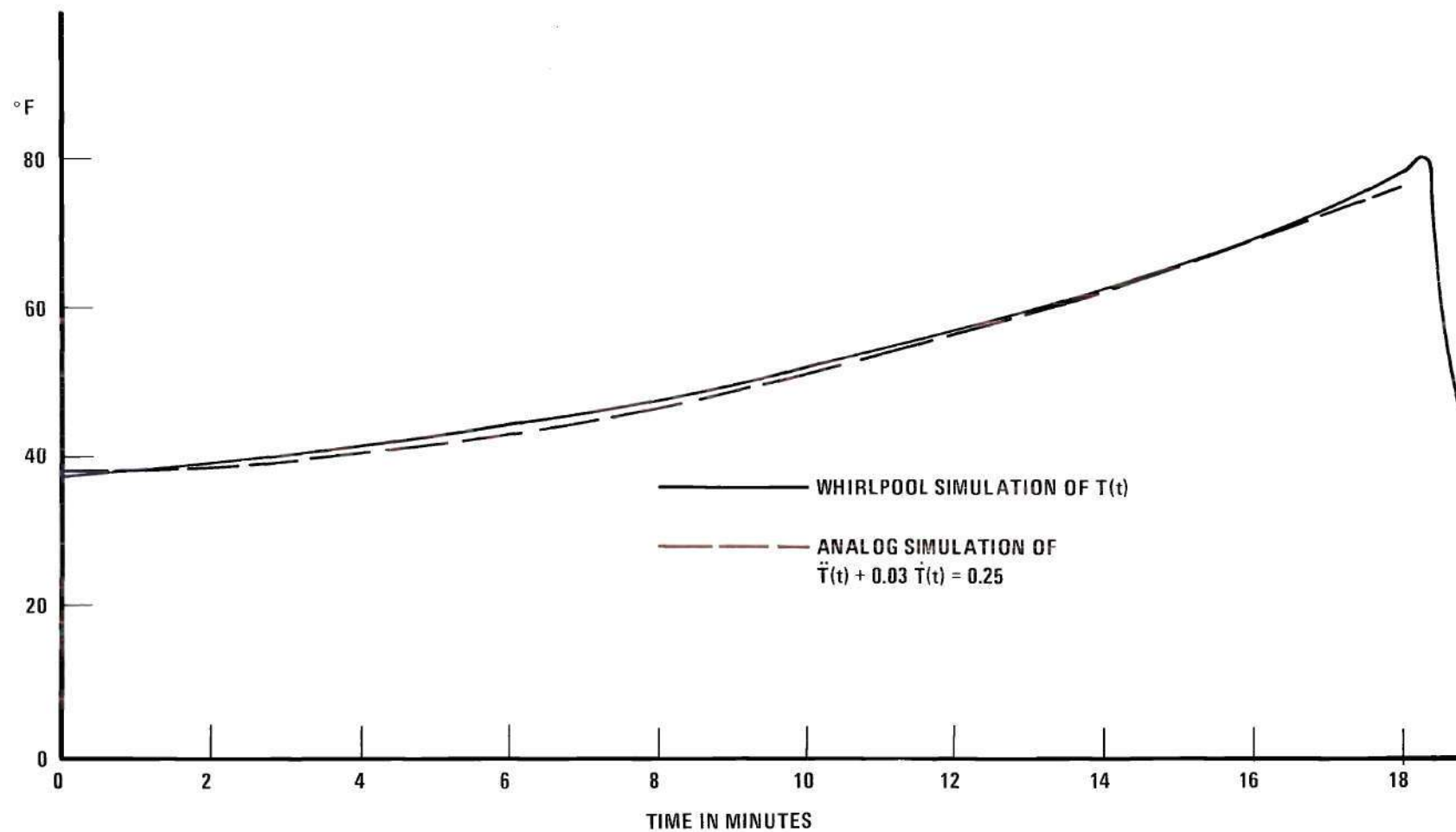


Figure 9. Comparison Between  $T(t)$  in Whirlpool Simulation and Analog Simulation of Heating Equation.

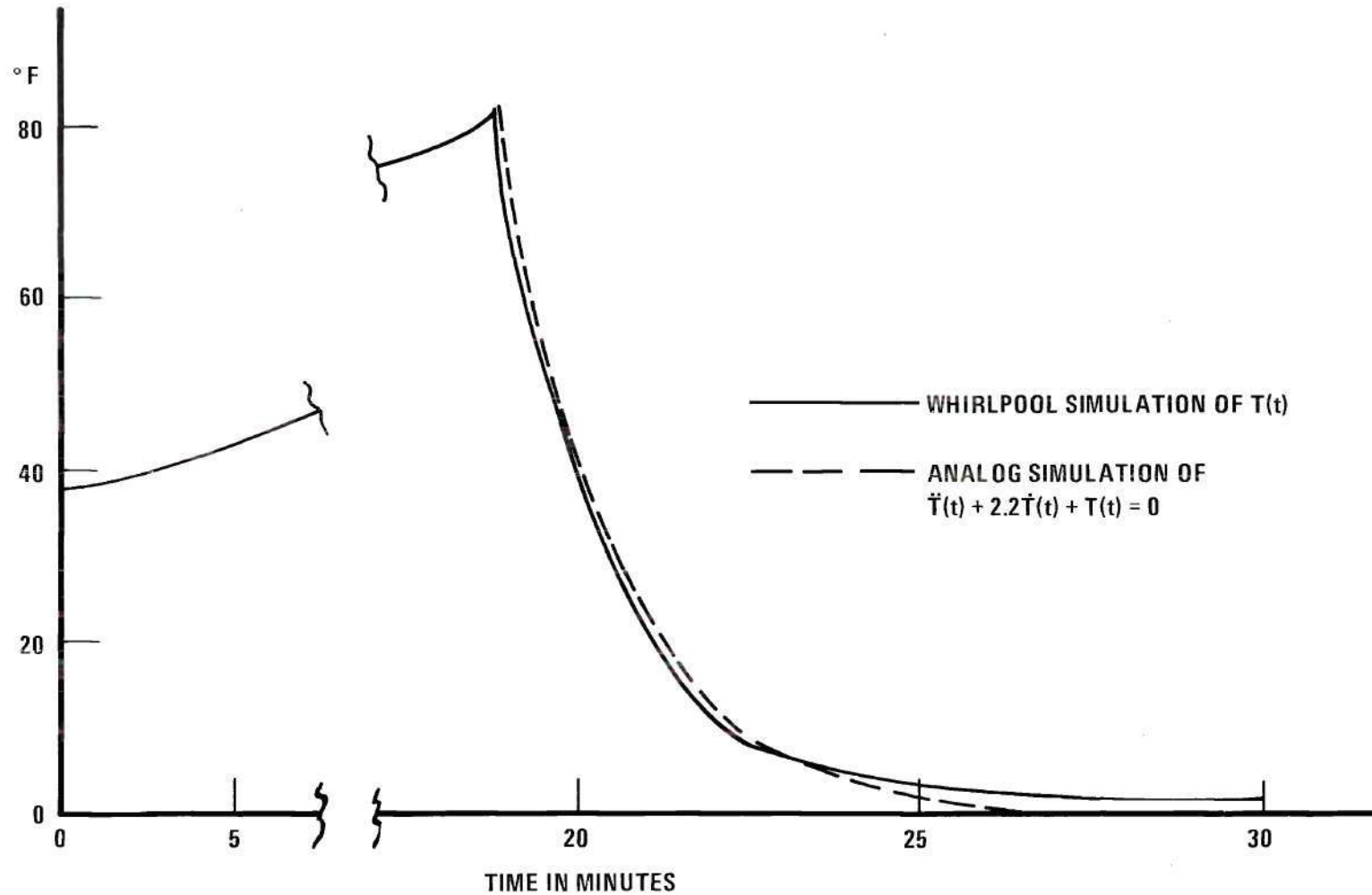
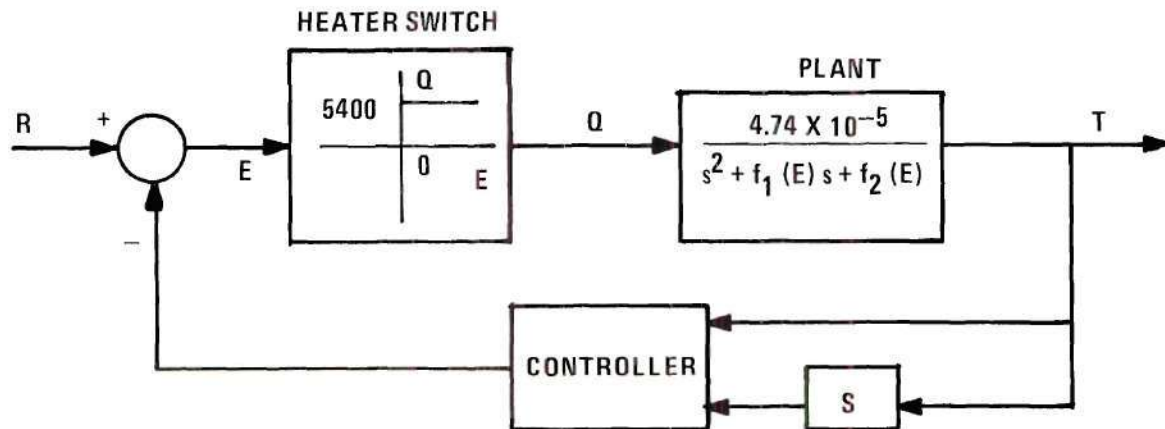


Figure 10. Comparison Between  $T(t)$  in Whirlpool Simulation and Analog Simulation of Cooling Equation.

point can be summarized in Figure 11, which presents the known plant equation and the still undetermined controller in a total system block diagram.

### Summary

A mathematical model for the heating-cooling system of the Whirlpool clothes dryer is determined for a nominal set of operating conditions. The model consists of two different linear time-invariant second-order differential equations, one of which is valid in the heating region, the other in the cooling region. Analog computer results verify the accuracy of the model, which is used in Chapter III to design an optimal controller for the dryer.



$$f_1(E) = \begin{cases} 2.2, & \text{if } E \geq 0 \\ 0.03, & \text{if } E < 0 \end{cases}$$

$$f_2(E) = \begin{cases} 0, & \text{if } E \geq 0 \\ 1, & \text{if } E < 0 \end{cases}$$

$R$  = Reference Temperature

$E$  = Error Signal

$Q$  = Electric Power of Heater

$T$  = Difference Between Exhaust Temperature and Assumed Room Temperature of  $70^\circ\text{F}$

$s$  = Laplace Transform Operator

Figure 11. System Block Diagram with Mathematical Model of Plant.

## CHAPTER III

### OPTIMAL CONTROL STRATEGY

#### Introduction

The objective of Chapter III is the design of a minimum time controller for the previously determined plant equation. Specifically, it is desired to increase the dryer's exhaust temperature from room temperature, when the dryer is initially turned on, to  $150^{\circ}$  F in the minimum time possible. The heater for the problem must be dual mode, i. e. it is constrained to be either full on at 5400 watts or full off. It is further desired that the exhaust temperature not overshoot  $150^{\circ}$  F.

The first step in the design of the optimal controller involves the simulation of the heating-cooling system of the dryer on an analog computer. Since the plant equation derived in Chapter II is second order, the analog computer can be programmed to provide two dimensional phase plane plots for various heating and cooling trajectories. From these trajectories, it is possible to determine the optimal switching curve. After deriving an analytical expression for the switching curve, the design of the optimal controller can be completed.

#### Phase Plane

Phase plane plots of the state variables  $T(t)$  and  $\dot{T}(t)$  can be obtained by a slight modification to the analog computer circuit of Figure 8. The modified circuit is shown in Figure 12. The resulting phase plane trajectories are depicted in Figure 13. The heating curves

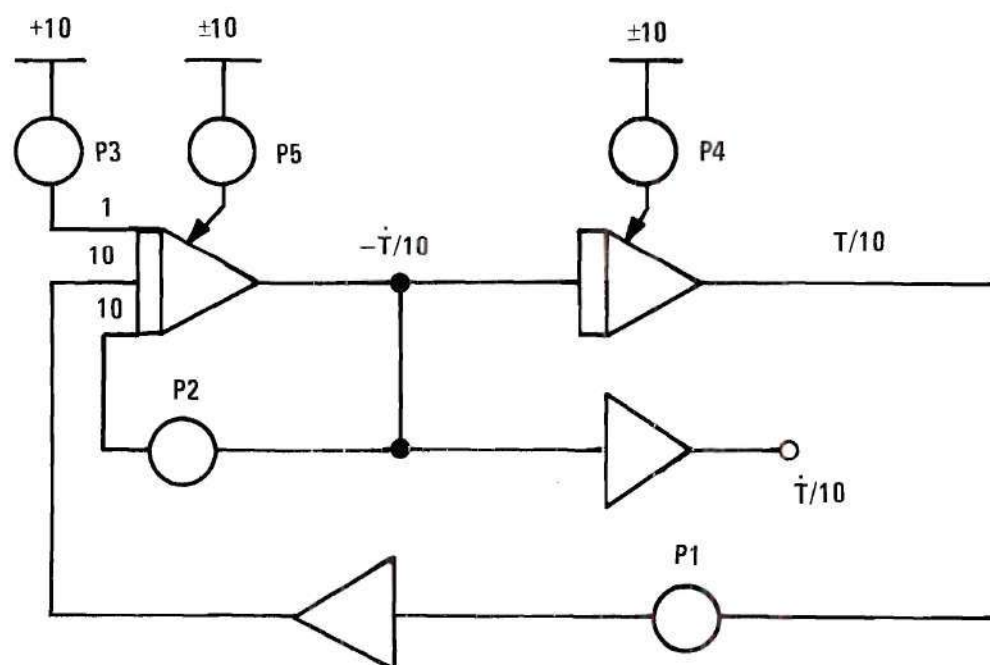


Figure 12. Analog Computer Circuit for Phase Plane Plots.



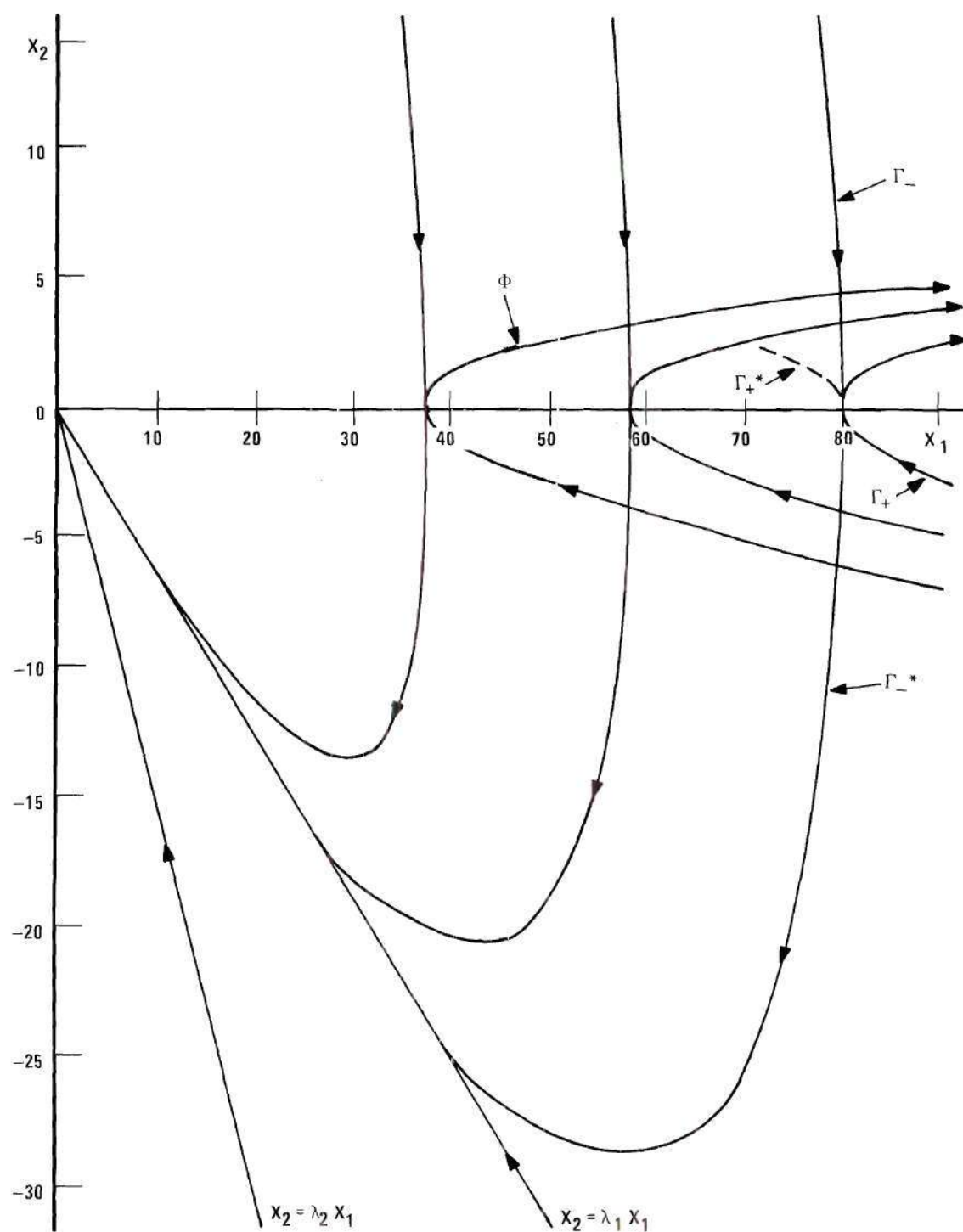


Figure 13. Phase Plane for Heating and Cooling Equations.

are obtained by programming

$$\ddot{T}(t) + 0.03 \dot{T}(t) = 4.74 \times 10^{-5} Q(t), \quad (2.5)$$

the heating equation derived in Chapter II. Potentiometer P1 is set to zero, P2 to .03, P3 to .0575 and P4 and P5 to various initial conditions.

The cooling curves, which all terminate at the assumed room temperature of 70° F, are obtained by programming

$$\ddot{T}(t) + 2.2 \dot{T}(t) + T(t) = 0, \quad (2.6)$$

the cooling equation of Chapter II. Potentiometer P1 is set to .1, P2 to .22, P3 to zero and P4 and P5 to various initial conditions.

#### Optimal Switching Curve

The objective is to drive the system state vector from

$$\begin{aligned} x_1(0) &= 37.5 \\ x_2(0) &= 0 \end{aligned} \quad (3.1)$$

to

$$\begin{aligned} x_1(t_f) &= 80.0 \\ x_2(t_f) &= 0 \end{aligned} \quad (3.2)$$

in the minimum time. The state variables are defined as

$$\begin{aligned} x_1(t) &= T(t) \\ x_2(t) &= \dot{T}(t) \end{aligned} \quad (3.3)$$

The initial value of  $\underline{x}$  is obtained from the first entry in Table 2 or Figure 6. The final value represents an exhaust temperature of  $150^{\circ}\text{F}$  with no overshoot. Observation of Figure 13 reveals that the only way to reach the final state  $\underline{x}(t_f)$  is along curves  $\Gamma_+$  or  $\Gamma_-$ . The strategy is to force the system along curve  $\Phi$  until the state reaches  $\Gamma_-$ . At this point, the input should be removed to allow the system to "coast" to  $\underline{x}(t_f)$  along  $\Gamma_-$ . The intersection of  $\Gamma_-$  and  $\Phi$  provides the necessary switching information.

Similarly, if the exhaust temperature were too high, the phase plane reveals that the optimum strategy for reaching  $150^{\circ}\text{F}$  is to turn the heater off until the state drifts down to the curve  $\Gamma_+$ . The heater should then be turned full on, bringing the state to  $\underline{x}(t_f)$ . It is obvious then that the optimum switching curve is the combination  $\Gamma_+$  and  $\Gamma_-$ . It is now desirable to determine the equation for the first half of the optimal switching curve, namely  $\Gamma_-$ . The curve  $\Gamma_-$  is a trajectory of the cooling equation

$$\ddot{T}(t) + 2.2 \dot{T}(t) + T(t) = 0 \quad (2.6)$$

In phase variable form, (2.6) becomes

$$\dot{\underline{x}} = \begin{bmatrix} \dot{x}_1 \\ \dot{x}_2 \end{bmatrix} = \begin{bmatrix} 0 & 1 \\ -1 & -2.2 \end{bmatrix} \begin{bmatrix} x_1 \\ x_2 \end{bmatrix} = A \underline{x} \quad (3.4)$$

The eigenvalues of the system are readily attained from

$$|\lambda I - A| = \lambda^2 + 2.2\lambda + 1 = 0 \quad (3.5)$$

They are

$$\begin{aligned}\lambda_1 &= -0.64 \\ \lambda_2 &= -1.56\end{aligned}\tag{3.6}$$

It is possible to find a relationship between  $x_1$  and  $x_2$  without transforming to uncoupled equations. Equation (3.4) could be integrated backward in time from  $\underline{x}(t_f)$ . However, the following method insures a solution which is not transcendental.

In order to determine  $\Gamma_-$ , it is useful to introduce [15] the transformation  $\underline{z} = M^{-1} \underline{x}$  or, more specifically

$$\begin{bmatrix} z_1 \\ z_2 \end{bmatrix} = \begin{bmatrix} -\lambda_2 & 1 \\ -\lambda_1 & 1 \end{bmatrix} \begin{bmatrix} x_1 \\ x_2 \end{bmatrix}\tag{3.7}$$

where  $M$  is the modal matrix. The  $z_1$  and  $z_2$ -axes are the straight line trajectories or separatrices shown in Figure 13. Thus the  $z_1 z_2$ -plane is a distortion of the  $x_1 x_2$ -plane. Using the transformation of (3.7) and the matrix equation  $\dot{\underline{z}} = M^{-1} A M \underline{z}$ , where  $A$  consists of eigenvalues on the main diagonal and zeros elsewhere, (3.4) can be uncoupled as

$$\begin{aligned}\dot{z}_1 &= \lambda_1 z_1 \\ \dot{z}_2 &= \lambda_2 z_2\end{aligned}\tag{3.8}$$

Elimination of time as a variable yields

$$\frac{dz_2}{z_2} = \frac{\lambda_2}{\lambda_1} \frac{dz_1}{z_1}\tag{3.9}$$

Therefore, all trajectories in the  $z_1 z_2$ -plane are described by

$$z_2 = c(z_1)^{\lambda_2/\lambda_1} \quad (3.10)$$

The constant term  $c$  may be determined for the specific case of the  $\Gamma_-$  curve by noting that the optimal trajectory passes through the state  $\underline{x}(t_f)$ . In the  $z_1 z_2$ -plane, this corresponds to

$$\begin{aligned} z_1(t_f) &= 124.8 \\ z_2(t_f) &= 51.2 \end{aligned} \quad (3.11)$$

Solving (3.10) for the unknown constant  $c$  gives

$$c = 0.0003 \quad (3.12)$$

The equation containing  $\Gamma_-$  is therefore

$$z_2 = 0.0003 z_1^{2.4} \quad (3.13)$$

However,  $\Gamma_-$  is only a subset of this trajectory since (3.13) consists of both  $\Gamma_-$  and  $\Gamma_-^*$  as shown in Figure 13. Substitution of an additional point on  $\Gamma_-$  reveals that the switching curve is defined by (3.13) with the added constraint that  $z_1 > 124.8$  and  $z_2 > 51.2$ .

To determine the equation of the switching curve  $\Gamma_+$ , consider the heating system

$$\ddot{T}(t) + 0.03 \dot{T}(t) = 4.74 \times 10^{-5} Q(t) \quad (2.5)$$

In state variable form,

$$\begin{bmatrix} \dot{x}_1 \\ \dot{x}_2 \end{bmatrix} = \begin{bmatrix} 0 & 1 \\ 0 & -\alpha \end{bmatrix} \begin{bmatrix} x_1 \\ x_2 \end{bmatrix} + \begin{bmatrix} 0 \\ 4.74 \times 10^{-5} \end{bmatrix} Q(t) = Ax + bQ \quad (3.14)$$

where  $\alpha = 0.03$ . Let  $Q(t)$  be constrained [16] such that  $-5400 \leq Q(t) \leq 5400$ . While  $Q(t)$  can only be 5400 watts in (2.5), it is convenient to assume the preceding limit in order to use the Maximum Principle of Pontryagin and derive an equation which is not transcendental. In the final analysis, only those trajectories for which  $Q(t) = 5400$  will be considered in the determination of  $\Gamma_+$ . The Hamiltonian is

$$H[x(t), Q(t), \lambda(t)] = 1 + \lambda^T(t) A x(t) + \lambda^T(t) b Q(t) \quad (3.15)$$

The Maximum Principle requires the minimization of the Hamiltonian with respect to a choice of  $Q(t)$ , so

$$Q(t) = -5400 \operatorname{sign} [\lambda^T(t) b] \quad (3.16)$$

Thus the Hamiltonian with the control optimum is

$$H[x(t), \lambda(t)] = 1 + \lambda^T(t) A x(t) - 5400 |\lambda^T(t) b| \quad (3.17)$$

Since the terminal time is free and since  $H$  does not depend explicitly on  $t$ ,

$$H[x(t), \lambda(t)] = 0, \quad \forall t \in [t_0, t_f] \quad (3.18)$$

on the optimal trajectory. The canonic equations are



$$\dot{x} = H_\lambda = A x(t) + b Q(t) = A x(t) - 5400 b \operatorname{sign} [\lambda^T(t) b] \quad (3.19)$$

$$\lambda = - H_{\lambda x} = - A^T \lambda(t) \quad (3.20)$$

The solution to the second canonic equation is

$$\lambda(t) = e^{-A(t-t_f)} \lambda(t_f) \quad (3.21)$$

It is convenient to rewrite the first canonic equation in terms of the time to go by letting  $t_0 = 0$  and

$$\tau = t_f - t \quad (3.22)$$

$$\xi(\tau) = x(t) = x(t_f - \tau) \quad (3.23)$$

This gives

$$\frac{d\xi}{d\tau} = -A \xi(\tau) + 5400 b \operatorname{sign} [\lambda^T(t_f) e^{A\tau} b] \quad (3.24)$$

which has as its solution

$$\xi(\tau) = \int_0^\tau e^{-A(\tau-p)} 5400 b \operatorname{sign} [\lambda^T(t_f) e^{A p} b] dp \quad (3.25)$$

since

$$\xi(0) = x(t_f) = 0.$$

For the problem at hand, it is a simple matter to compute the state transition matrix as

$$e^{A t} = \begin{bmatrix} 1 & \frac{1}{\alpha}(1 - e^{-\alpha t}) \\ 0 & e^{-\alpha t} \end{bmatrix} \quad (3.26)$$

and the equation for the switching boundary as

$$\begin{aligned} \xi(\tau_s) &= \begin{bmatrix} 1 & \frac{1}{\alpha}(1 - e^{\alpha \tau_s}) \\ 0 & e^{\alpha \tau_s} \end{bmatrix} \int_0^{\tau_s} \begin{bmatrix} \frac{1}{4\alpha}(1 - e^{-\alpha p}) \\ \frac{1}{4} e^{-\alpha p} \end{bmatrix} \\ &\cdot \text{sign} \left\{ \lambda_1(t_f) \left[ \frac{1}{4\alpha} (1 - e^{-\alpha p}) \right] + \lambda_2(t_f) \frac{e^{-\alpha p}}{4} \right\} dp \end{aligned} \quad (3.27)$$

Upon evaluation of this expression, the switching boundary is given by the equation

$$x_1(t) + \frac{1}{\alpha} x_2(t) - \left\{ \frac{\text{sign} [x_2(t)]}{\alpha^2} \right\} \ln [1 + \alpha |x_2(t)|] = 0 \quad (3.28)$$

The equation for  $\Gamma_+$  however is actually a translated subset of (3.28). Translating (3.28) from the origin to  $\underline{x}(t_f)$  results in  $\Gamma_+$  and  $\Gamma_+^*$  in Figure 13. The exact equation for the second half of the optimal switching curve, i. e.  $\Gamma_+$  is

$$x_1(t) - 80 + 33.3 x_2(t) + 1089 \ln [1 + 0.03 |x_2(t)|] = 0 \quad (3.29)$$

with the additional constraint that  $x_2 \leq 0$ .

### Optimal Controller

It is now possible to design the block diagram for the optimal controller by utilizing the previously derived equations for the

optimal switching curve. The basic strategy is to determine whether the present state is to the left or to the right of the optimal switching curve in Figure 13. If the state is to the left, then the heater should be turned on. On the other hand, if the state is to the right, the heater should be off.

The complete system block diagram containing the optimal controller is shown in Figure 14. The error signal  $E$  controls the heater switch which is modeled as an ideal relay. If  $E$  is greater than zero, then 5400 watts is applied to the heater. On the other hand, if  $E$  is less than zero, no power is applied to the heater. Writing the plant equation of Figure 11 in state variable form results in

$$\begin{bmatrix} \dot{x}_1 \\ \dot{x}_2 \end{bmatrix} = \begin{bmatrix} 0 & 1 \\ f_2(E) & f_1(E) \end{bmatrix} \begin{bmatrix} x_1 \\ x_2 \end{bmatrix} + \begin{bmatrix} 0 \\ b_0 \end{bmatrix} Q(t) \quad (3.30)$$

where

$$f_1(E) = \begin{cases} 2.2, & \text{if } E \geq 0 \\ 0.03, & \text{otherwise} \end{cases} \quad (3.31)$$

$$f_2(E) = \begin{cases} 0, & \text{if } E \geq 0 \\ 1, & \text{otherwise} \end{cases} \quad (3.32)$$

$$b_0 = 4.74 \times 10^{-5} \quad (3.33)$$

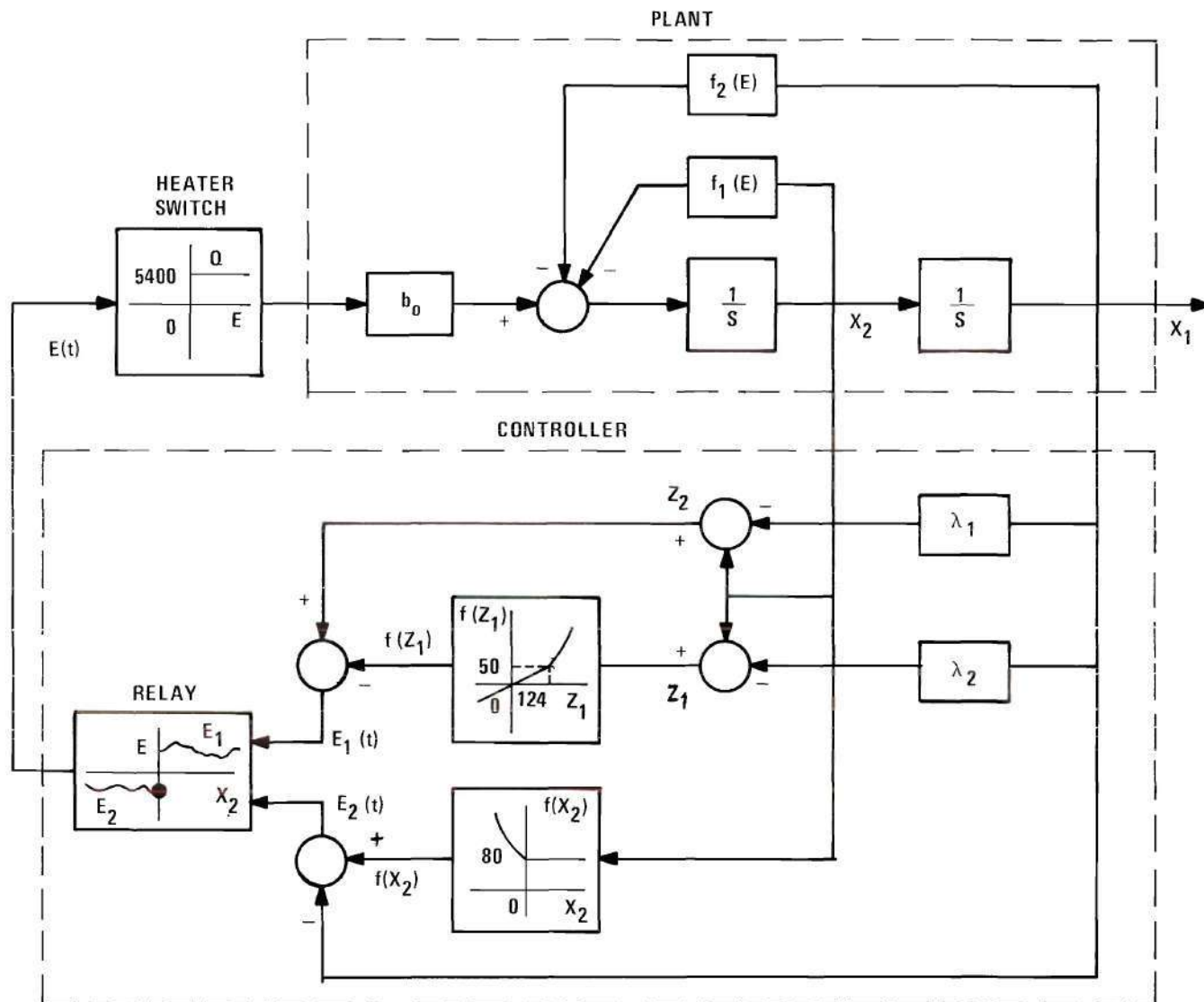


Figure 14. Optimal Control System Block Diagram.

In Figure 14, the portion of the block diagram representing the plant follows directly from (3.30). Since  $\Gamma_-$  is defined in terms of uncoupled  $z$  state variables, the first task of the controller is the determination of  $z_1$  and  $z_2$ . This is easily accomplished by programming (3.6) and (3.7).

The main elements of the controller consist of the instrumentation required to compute the complex nonlinear optimal switching curve. This is accomplished by the functions  $f(z_1)$  and  $f(x_2)$  which are defined as

$$f(z_1) = \begin{cases} 0.0003 z_1^{2.4} & , \quad z_1 \geq 124.8 \\ 0.415 z_1 & , \quad z_1 < 124.8 \end{cases} \quad (3.34)$$

$$f(x_2) = \begin{cases} 80 - 33.3 x_2 - 1089 \ln [1 + 0.03 |x_2|], & x_2 \leq 0 \\ 0 & , \quad x_2 > 0 \end{cases} \quad (3.35)$$

The line

$$f(z_1) = 0.415 z_1 \quad (3.36)$$

where  $z_1 < 124.8$  is the linear transformation of the line

$$x_2 = 0$$

where  $x_1 < 0$ . The final element of the controller is the relay which defines the error signal  $E$  as

$$E(t) = \begin{cases} E_1(t) = z_2 - f(z_1), & x_2 > 0 \\ E_2(t) = f(x_2) - x_1, & x_2 \leq 0 \end{cases} \quad (3.37)$$

In the  $z$ -plane (3.5) gives the initial conditions as

$$\begin{aligned} z_1(0) &= 58.4 \\ z_2(0) &= 24.0 \end{aligned} \quad (3.8)$$

The error signal is initially

$$E(0) = f[x_2(0)] - x_1(0) = 42.5 \quad (3.39)$$

so the heater is switched on. At time  $t = \delta$  where  $\delta$  is very small but greater than zero, the phase plane of Figure 13 indicates that  $x_2(\delta) > 0$ . Specifically

$$\begin{aligned} x_1(\delta) &= 37.5 + \epsilon_1 = 37.5 \\ x_2(\delta) &= \epsilon_2 \end{aligned} \quad (3.40)$$

where  $\epsilon_2 \gg \epsilon_1 > 0$  for sufficiently small  $\delta$ . Thus at  $t = \delta$  the controller relay switches to

$$E(\delta) = z_2(\delta) - f[z_1(\delta)] \quad (3.41)$$

Equation (3.7) reveals that

$$\begin{aligned} z_1(\delta) &= 58.4 + \epsilon_2 \\ z_2(\delta) &= 24.0 + \epsilon_2 \end{aligned} \quad (3.42)$$

The controller utilizes (3.34) next to calculate

$$f[z_1(\delta)] = 0.415 z_1(\delta) = 24.2 + 0.415 \epsilon_2 \quad (3.43)$$

The error signal is then

$$E(\delta) = 0.415 \epsilon_2 \quad (3.44)$$

so the heater remains on.

The error signal remains positive until the curve  $\Phi$  intersects the optimal switching curve  $\Gamma_+$ . This occurs at  $t = t_s = 18.3$  minutes with

$$\begin{aligned} x_1(t_s) &= 79.8 \\ x_2(t_s) &= 4.15 \end{aligned} \quad (3.45)$$

and

$$\begin{aligned} z_1(t_s) &= 128.2 \\ z_2(t_s) &= 56.4 \end{aligned} \quad (3.46)$$

This time  $z_1 > 124.8$  so (3.34) yields

$$f[z_1(t_s)] = 0.0003 z_1^{2.4} = 56.4 \quad (3.47)$$

The error signal is still given by

$$E(t_s) = z_2 - f(z_1) = 0 \quad (3.48)$$

and as a result, the heater shuts off. The heater remains turned off until  $\Gamma_-$  reaches the desired state  $\underline{x}(t_f)$  at which time the controller relay switches back to  $f(x_2)$ .



$$f(x_2 = 0) = 80 \quad (3.49)$$

Error is now defined as

$$E = f(x_2) - x_1 = 0 \quad (3.50)$$

The control system now switches the heater on and off at a theoretically infinite rate of frequency. This condition is referred to in the literature as relay chatter. Since it is physically impossible to design a device which switches in zero time, it is not possible to implement the optimal controller exactly.

### Sensitivity Analysis

The mathematical model derived in Chapter II is based on the unique set of data in Table 1. At that time it was postulated that the model would be sufficiently accurate for operating conditions in the vicinity of the Table 1 data. It is now appropriate to examine this hypothesis and determine the performance of the optimal controller when certain parameters in Table 1 are varied.

In the first case, a four pound (dry) clothes load with 75 per cent initial moisture content is considered. The remaining parameters are identical to Table 1. The steady-state exhaust temperature for this case is  $130.1^{\circ}\text{F}$ . The trajectory predicted by the mathematical model is shown in Figure 15. Upon reaching the optimal switching curve  $\Gamma_*$ , the heater shuts off and the state should move to  $\underline{x}(t_f)$ . According to the Whirlpool Dryer simulation, the state moves along a slightly different curve. The heater switches off when the state

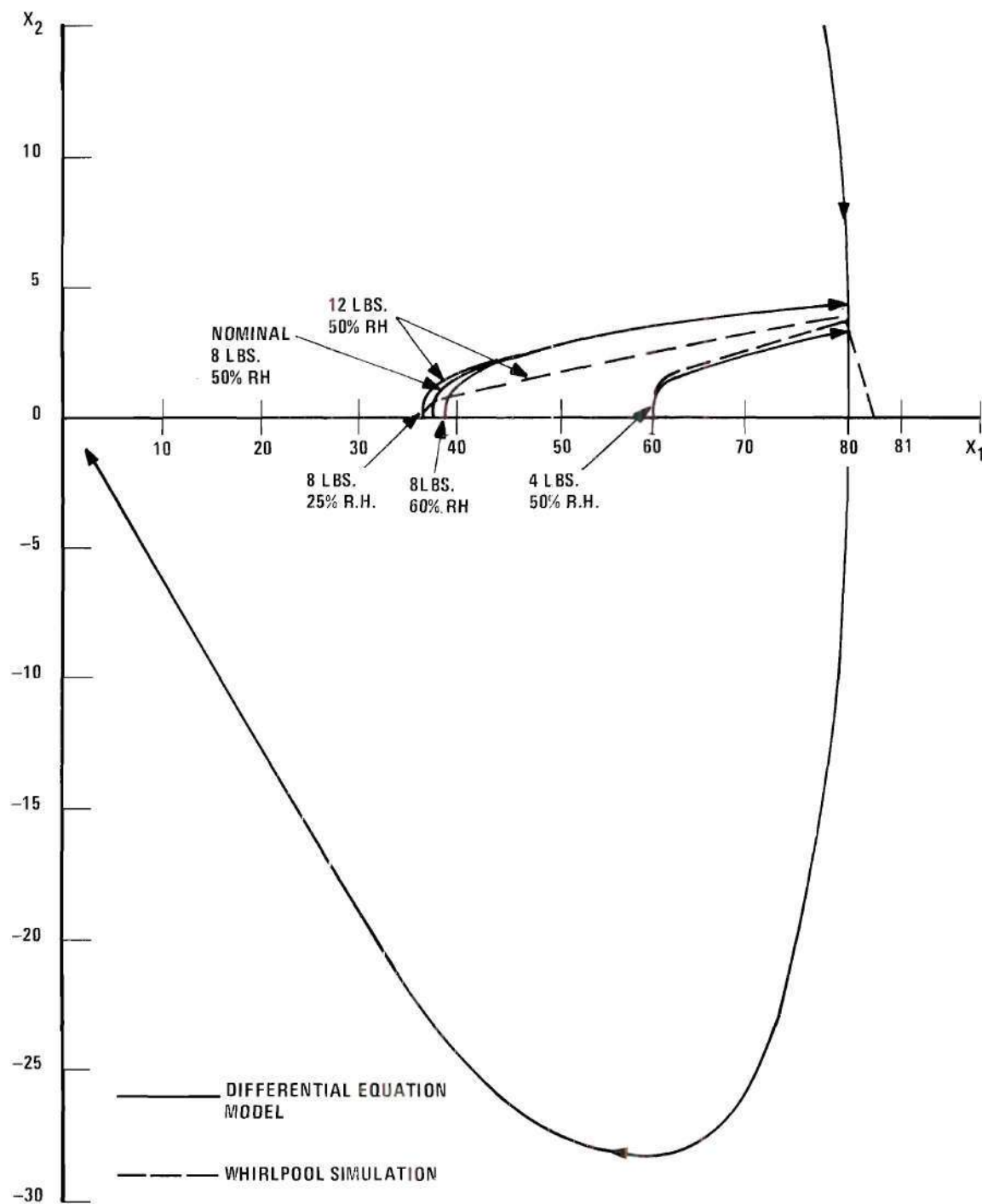


Figure 15. Deviations in Phase Plane Trajectories Resulting from Parameter Variations.

reaches  $\Gamma_-$ . However, the state then proceeds to

$$\begin{aligned}x_1(t_f) &= 80.6 \\x_2(t_f) &= 0\end{aligned}\tag{3.51}$$

Thus the optimal controller errs by the relatively small margin of  $0.6^\circ \text{ F}$ .

In the second case, a 12 pound clothes load with 75 per cent initial moisture content is evaluated. Again the remaining parameters are unchanged. This time the steady-state temperature is  $104.5^\circ \text{ F}$ . As Figure 15 indicates, the difference between transient states is somewhat greater. The controller, however, still moves the state to

$$\begin{aligned}x_1(t_f) &= 80.5 \\x_2(t_f) &= 0\end{aligned}\tag{3.52}$$

Two additional cases consider the effects of a change in the relative humidity. For both 25 per cent and 60 per cent relative humidity the optimal controller translates the state to

$$\begin{aligned}x_1(t_f) &= 81.0 \\x_2(t_f) &= 0\end{aligned}\tag{3.53}$$

in minimum time. These four cases tend to support the hypothesis that the optimal controller performs adequately under reasonable operating conditions.

### Summary

In Chapter III, a plot of phase plane trajectories is acquired by means of an analog computer simulation. From this phase plane plot, the optimal switching curve is determined both graphically and analytically. With the added knowledge of a nontranscendental optimal switching curve equation, it is then possible to design the optimal controller.

In Chapter II, a mathematical model of the plant is developed for a typical clothes load under typical operating conditions, i. e. eight pound permanent press load with 50 per cent relative humidity and 70° F room temperature. In the final section of Chapter III, the performance of the optimal controller is evaluated for different loads and different operating conditions. In conclusion, the drawback to optimal control is in complexity and in physical unrealizability. An attempt at remedying this situation is found in Chapter IV wherein a less complex, suboptimal controller is presented.

## CHAPTER IV

### SUBOPTIMAL CONTROL STRATEGY

#### Introduction

In Chapter IV, a practical suboptimal controller is presented which overcomes the objections to the optimal controller derived in Chapter III. While any suboptimal controller, by definition, does not perform as well as the optimal controller, the nature of the control problem under consideration in this thesis is such that a suboptimal strategy exists which essentially performs as well as the optimal strategy. The reason is that the region of the phase plane through which potential trajectories traverse is quite limited. For instance, at the beginning of the falling-rate region of operation, the exhaust temperature  $T_E$  should be between  $100^{\circ}\text{F}$  and  $150^{\circ}\text{F}$ . The rate of change of exhaust temperature  $\dot{T}_E$  should be zero. All trajectories then move into the fourth quadrant before switching and moving into the vicinity of  $\underline{x}(t_f)$ . The prospect of confinement to a limited region of operation in the state plane suggests linearizing the optimal switching curve about a nominal trajectory. This leads to a proportional-plus-derivative control system.

#### Proportional-Plus-Derivative Switching Curve

A proportional-plus-derivative switching curve consists of a straight line passing through the desired final state  $\underline{x}(t_f)$ . The slope of the line is chosen such that the proportional-plus-derivative



switching curve closely approximates the optimal switching curve in some localized region of the phase plane. In Figure 13, the trajectory  $\bar{\Phi}$  is considered to be a typical or average trajectory since it corresponds to the typical dryer parameters of Table 1. In Figure 16,  $\bar{\Phi}$  intersects the optimal switching curve  $\Gamma_-$  at

$$\begin{aligned}x_1(t_s) &= 79.8 \\x_2(t_s) &= 4.15\end{aligned}\tag{4.1}$$

If a straight line is drawn between  $\underline{x}(t_s)$  and the desired final state  $\underline{x}(t_f)$ , the proportional-plus-derivative switching curve  $\gamma$  results. Since  $\underline{x}(t_s)$  is on both  $\Gamma_-$  and  $\gamma$ , the suboptimal curve  $\gamma$  is optimal for the case of trajectory  $\bar{\Phi}$ . As trajectories deviate from  $\bar{\Phi}$ , the performance of the suboptimal switching curve deteriorates slightly in proportion to the degree of deviation from  $\bar{\Phi}$ . However, since  $\bar{\Phi}$  represents an average trajectory, it is reasonable to expect all trajectories to be close to  $\bar{\Phi}$  and hence all performances close to optimal.

To make the analysis more practical, consider a heater switch with a hysteresis loop equal to  $\theta^\circ$  F. For a tolerance of  $\pm 1^\circ$  F, the heater shuts off when  $\gamma_-$  is crossed from left to right as shown in Figure 16. Similarly, the heater turns on when  $\gamma_+$  is crossed from right to left. Thus, after traversing  $\bar{\Phi}$  and  $\beta$ , the state enters a limit cycle. The state variable  $x_1$  then remains within the interval

$$79.0 \leq x_1(t) \leq 81.0\tag{4.2}$$



48



### Proportional-Plus-Derivative Controller

A suboptimal controller which meets the specified tolerance of  $\pm 1^\circ \text{ F}$  for the nominal conditions of Table 1 is depicted in Figure 17. Figure 16 reveals that it is necessary to have a heater switch with a hysteresis parameter

$$\theta \leq 0.08 \quad (4.3)$$

to meet the specification. The reference input signal should be set to

$$R = 80.96 \quad (4.4)$$

The value of  $K_D$  is equivalent to the reciprocal of the slope of  $\gamma$  in Figure 16 or

$$K_D = 0.048 \quad (4.5)$$

For the nominal parameters of Table 1, the state traverses curve  $\Phi$  as before. This time, the heater does not shut off until reaching the point

$$\begin{aligned} x_1(t_s) &= 80.8 \\ x_2(t_s) &= 4.15 \end{aligned} \quad (4.6)$$

on  $\gamma_-$ . The system cools along  $\beta$  and heats along  $\Phi_1$ . This is a limit cycle wherein the exhaust temperature varies between  $149^\circ \text{ F}$  and  $151^\circ \text{ F}$ .

The duration of the cycle and the percent-on time can be determined from the simple equality

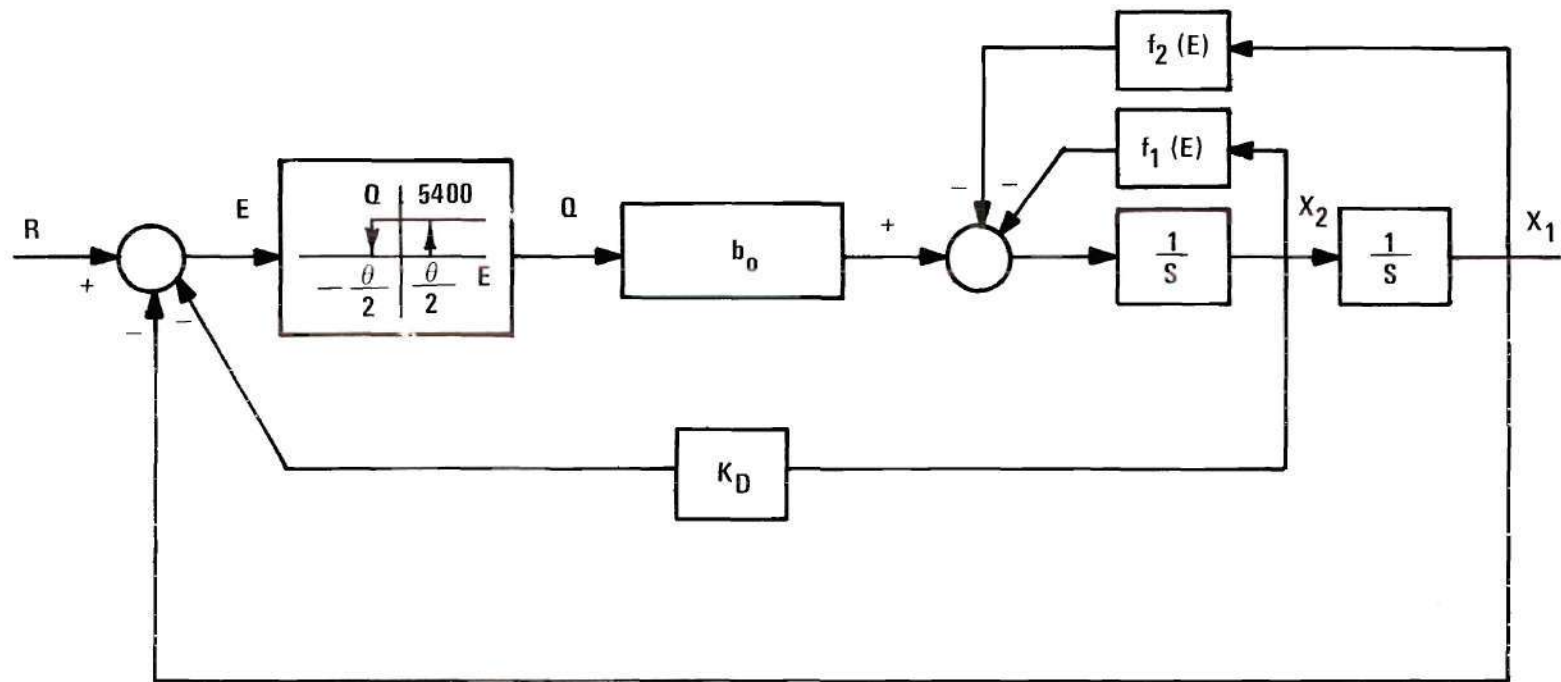


Figure 17. Suboptimal Proportional-Plus-Derivative Control System Block Diagram.

$$\Delta t = \frac{\Delta x_1}{\bar{x}_2} \quad (4.7)$$

where  $\Delta t$  is the time interval to be determined. If the state is at  $(x_{10}, x_{20})$  initially and at  $(x_{11}, x_{21})$   $\Delta t$  minutes later, then

$$\Delta x_1 = x_{11} - x_{10} \quad (4.8)$$

and

$$\bar{x}_2 = \frac{x_{20} + x_{21}}{2} \quad (4.9)$$

The resulting period of the limit cycle is

$$t_p = 5 \text{ minutes } 45 \text{ seconds} \quad (4.10)$$

Heating and cooling times are

$$t_H = 5 \text{ minutes } 30 \text{ seconds}$$

$$t_C = 15 \text{ seconds} \quad (4.11)$$

respectively. The per cent-on time is therefore

$$\frac{t_H}{t_p} = 96 \text{ per cent} \quad (4.12)$$

### Sensitivity Analysis

The sensitivity of temperature control to variations in relative humidity and clothes load is evaluated with the aid of the Whirlpool simulation program. In particular, the ability of the suboptimal

controller to regulate the exhaust temperature for five different sets of operating conditions is determined.

In the first case, the relative humidity in Table 1 is increased to 60 per cent while other parameters remain unchanged. The Whirlpool simulation reveals that the exhaust temperature cycles between  $146^{\circ}$  F and  $152^{\circ}$  F after initially reaching  $150^{\circ}$  F.

In the second case, the relative humidity is lowered to 25 per cent. The exhaust temperature then cycles between  $144^{\circ}$  F and  $154^{\circ}$  F.

In the third case, the relative humidity is set at 75 per cent. However, the clothes load dries completely before the exhaust temperature even reaches  $150^{\circ}$  F. Thus, there is no control problem.

For the fourth case, the relative humidity is returned to the nominal value of 50 per cent and the clothes load weight is increased to twelve pounds. The exhaust temperature ranges between  $149^{\circ}$  F and  $154^{\circ}$  F.

In the final case, a four-pound clothes load is considered. This time the exhaust temperature cycles between  $137^{\circ}$  F and  $152^{\circ}$  F. Since this represents the worst case, it is desirable to compare these results with those of the present production proportional control system with a  $15^{\circ}$  F thermostatic differential. The current system cycles between  $124^{\circ}$  F and  $158^{\circ}$  F. Although the suboptimal controller designed herein does not control to  $\pm 1^{\circ}$  F for all parameter variations, it does represent an improvement over the present controller.

#### Summary

In Chapter IV, the optimal switching curve is linearized about a

nominal trajectory in order to simplify the optimal controller. This results in a proportional-plus-derivative control system. The proportional-plus-derivative controller is evaluated for various dryer clothes loads under various operating conditions. It is found to perform reasonably well. The chief advantage of the suboptimal proportional-plus-derivative controller over the optimal controller lies in its comparative simplicity and hence in its comparative cost.

## CHAPTER V

### CONCLUSIONS AND RECOMMENDATIONS

#### Conclusions

A mathematical model is developed to simulate the exhaust temperature in the falling-rate region for a nominal set of operating conditions. As these nominal conditions are varied, the model begins to lose accuracy. There exist certain pathological cases for which the model deviates significantly from reality. Most of these pathological cases, however, are not encountered during normal operation of the machine.

An optimal controller is designed on the basis of previously mentioned nominal conditions. The controller increases the exhaust temperature from an assumed room temperature of  $70^{\circ}\text{F}$  to  $150^{\circ}\text{F}$  in minimum time. Theoretically, the temperature then remains at  $150^{\circ}\text{F}$  as the heater switches on and off at an infinite rate of frequency. Parameter sensitivity studies indicate that variations in relative humidity and clothes load weight have minimal affect on system operation. In four out of five cases considered, the optimal controller translates the exhaust temperature to some value within the interval  $150^{\circ}\text{F} \pm 1^{\circ}\text{F}$  without overshoot and in minimum time.

There are two basic objections to the optimal controller. First, it is quite complex and hence quite costly. The implementation of the optimal switching curve would require some very sophisticated circuitry if not a minicomputer. Second, the optimal controller is physically



unrealizable since it requires a relay or triac which switches in zero time.

A suboptimal controller is designed to overcome these two objections. The controller system utilizes proportional-plus-derivative feedback as well as a switching relay or triac with hysteresis. Since the switching curves are linear, the resulting controller electronics would be considerably less complex than in the optimal case. Also, this controller is physically realizable because hysteresis is added to the heater switch. With this system, it is possible to increase the exhaust temperature to  $150^{\circ}\text{ F} \pm 1^{\circ}\text{ F}$  in minimum time and maintain that tolerance for the nominal case. A sensitivity analysis indicates that variations in relative humidity and clothes load weight increase this tolerance somewhat. However, comparison tests with a computer simulation of the current production proportional control system with a  $15^{\circ}\text{ F}$  thermostatic differential indicate that the suboptimal controller performs better.

### Recommendations

The design of any control system inherently requires an accurate mathematical model of the plant. In view of this, further research in the area should concentrate on developing a more accurate plant model. However, a model which is overly complex will result in either an overly complex controller or in a controller which is impossible to design. Therefore numerical analysis techniques could be utilized to develop nonlinear second-order equations wherein the constant coefficients in this thesis would become functions of the various parameters, i. e.



weight, relative humidity, etc. An alternative method would be to derive a theoretical model based on the thermodynamics of the system as the falling-rate region becomes more readily understood. At any rate, the powerful techniques of modern control theory should definitely be employed in the development of any improved controllers.

## APPENDIX

# LEAST-SQUARES CURVE FIT

It is desired to minimize the sum of least square errors

$$S = \sum_{n=1}^N (T_{\text{observed}} - T_{\text{equation}})^2 \quad (\text{A.1})$$

where  $N$  is the number of data points considered.  $T_{\text{equation}}$  is simply  $T(t)$  in equation (2.2) evaluated at discrete points in time

$$T_{\text{equation}} = -a_0 \ddot{T}_n - a_1 \dot{T}_n + b Q_n \quad (\text{A.2})$$

where  $\dot{T}_n$  and  $\ddot{T}_n$  are the first and second derivatives evaluated at the  $n$ th data point. Realizing that  $T_{\text{observed}}$  is equivalent to  $T_n$ , (A.2) can be substituted into (A.1) to yield

$$S = \sum_{n=1}^N (a_0 \ddot{T}_n + a_1 \dot{T}_n + T_n - b Q_n)^2 \quad (\text{A.3})$$

This sum can be minimized by taking the partial derivatives of  $S$  with respect to  $a_0$ ,  $a_1$ , and  $b$  and setting the result equal to zero, i. e.

$$\frac{\partial S}{\partial a_0} = 2 \sum_{n=1}^N (a_0 \ddot{T}_n + a_1 \dot{T}_n + T_n - b Q_n) \ddot{T}_n = 0 \quad (\text{A.4})$$

$$\frac{\partial S}{\partial a_1} = 2 \sum_{n=1}^N (a_0 \ddot{T}_n + a_1 \dot{T}_n + T_n - b Q_n) \dot{T}_n = 0 \quad (\text{A.5})$$

$$\frac{\partial S}{\partial b} = 2 \sum_{n=1}^N (a_0 \ddot{T}_n + a_1 \dot{T}_n + T_n - b Q_n) (-Q_n) = 0 \quad (A.6)$$

simplifying (A.4) through (A.6) yields

$$\sum \ddot{T}_n^2 a_0 + \sum \dot{T}_n \ddot{T}_n a_1 - \sum Q_n \ddot{T}_n b = - \sum T_n \ddot{T}_n \quad (A.7)$$

$$\sum \ddot{T}_n \dot{T}_n a_0 + \sum \dot{T}_n^2 a_1 - \sum Q_n \dot{T}_n b = - \sum T_n \dot{T}_n \quad (A.8)$$

$$- \sum \ddot{T}_n Q_n a_0 - \sum \dot{T}_n Q_n a_1 + \sum Q_n^2 b = \sum T_n Q_n \quad (A.9)$$

where all summations are from  $n=1$  to  $N$ . Equations (A.7) through (A.9) can be written in matrix notation

$$\begin{bmatrix} \sum \ddot{T}_n^2 & \sum \dot{T}_n \ddot{T}_n & - \sum Q_n \ddot{T}_n \\ \sum \ddot{T}_n \dot{T}_n & \sum \dot{T}_n^2 & - \sum Q_n \dot{T}_n \\ - \sum \ddot{T}_n Q_n & - \sum \dot{T}_n Q_n & \sum Q_n^2 \end{bmatrix} \begin{bmatrix} a_0 \\ a_1 \\ b \end{bmatrix} = \begin{bmatrix} - \sum T_n \ddot{T}_n \\ - \sum T_n \dot{T}_n \\ \sum T_n Q_n \end{bmatrix} \quad (A.10)$$

Solving (A.10) for the unknown coefficients  $a_0$ ,  $a_1$  and  $b$  results in

$$\begin{bmatrix} a_0 \\ a_1 \\ b \end{bmatrix} = \begin{bmatrix} \sum \ddot{T}_n^2 & \sum \dot{T}_n \ddot{T}_n & - \sum Q_n \ddot{T}_n \\ \sum \ddot{T}_n \dot{T}_n & \sum \dot{T}_n^2 & - \sum Q_n \dot{T}_n \\ - \sum \ddot{T}_n Q_n & - \sum \dot{T}_n Q_n & \sum Q_n^2 \end{bmatrix}^{-1} \begin{bmatrix} - \sum T_n \ddot{T}_n \\ - \sum T_n \dot{T}_n \\ \sum T_n Q_n \end{bmatrix} \quad (A.11)$$

The above derivatives can be approximated by appropriate difference equations. Consider the following Taylor series expansions:

$$\begin{aligned}
T(t \pm h) = T(t) \pm h \dot{T} + \frac{h^2}{2} \ddot{T} \pm \frac{h^3}{6} T^{(iii)} \\
+ \frac{h^4}{24} T^{(iv)} \pm \frac{h^5}{120} T^{(v)} + \dots
\end{aligned} \quad (A.12)$$

and

$$\begin{aligned}
T(t \pm 2h) = T(t) \pm 2h \dot{T} + 2h^2 \ddot{T} \pm \frac{4}{3} h^3 T^{(iii)} \\
+ \frac{2}{3} h^4 T^{(iv)} \pm \frac{4}{15} h^5 T^{(v)} + \frac{64}{720} h^6 T^{(vi)} \pm \dots
\end{aligned} \quad (A.13)$$

Then

$$T(t+h) - T(t-h) = 2h \dot{T} + \frac{h^3}{3} T^{(iii)} + \frac{h^5}{60} T^{(v)} + \dots \quad (A.14)$$

and

$$T(t+2h) - T(t-2h) = 4h \dot{T} + \frac{8}{3} h^3 T^{(iii)} + \frac{64}{120} h^5 T^{(v)} + \dots \quad (A.15)$$

Equations (A.14) and (A.15) can be combined to give

$$\begin{aligned}
T_{n+2} - 8T_{n+1} + 8T_{n-1} - T_{n-2} \\
= -12h \dot{T} + \frac{48}{120} h^5 T^{(v)} + \dots
\end{aligned} \quad (A.16)$$

where  $T_{n+a}$  is equivalent to  $T(t+ah)$ . Solving for  $\dot{T}$  in (A.16) results in

$$\dot{T} = \frac{-T_{n+2} + 8T_{n+1} - 8T_{n-1} + T_{n-2}}{12h} \quad (A.17)$$

which has a truncation error of  $\frac{48}{1440} h^4 T^{(iv)}$ .

The second derivative can be approximated in a similar manner.

Equations (A.12) and (A.13) lead to

$$T_{n+1} + T_{n-1} = 2 T_n + h^2 \ddot{T} + \frac{h^4}{12} T^{(iv)} + \frac{2 h^6}{720} T^{(vi)} + \dots \quad (A.18)$$

and

$$T_{n+2} + T_{n-2} = 2 T_n + 4 h^2 \ddot{T} + \frac{4}{3} h^4 T^{(iv)} + \frac{128}{720} h^6 T^{(vi)} + \dots \quad (A.19)$$

Combining (A.18) and (A.19) results in

$$\begin{aligned} T_{n+2} - 16 T_{n+1} + 30 T_n - 16 T_{n-1} + T_{n-2} \\ = -12 h^2 \ddot{T} + \frac{96}{720} h^6 T^{(vi)} + \dots \end{aligned} \quad (A.20)$$

Solving (A.20) for  $\ddot{T}$  yields

$$\ddot{T} = \frac{-T_{n+2} + 16 T_{n+1} - 30 T_n + 16 T_{n-1} - T_{n-2}}{12 h^2} \quad (A.21)$$

which has a truncation error of  $\frac{96}{8640} h^4 T^{(vi)}$ . The approximations of  $\dot{T}$  in (A.17) and  $\ddot{T}$  in (A.21) can be utilized in (A.11).

## BIBLIOGRAPHY

1. Hurley, R. B., "The Tumble-Drying Process and Acrylic Knitted Fabrics," Textile Research Journal, Vol. 9, pp. 746-51, September, 1967.
2. Fanson, R. and Tibbitts, W. I., "Model 433-M Clothes Dryer Heat and Mass Transfer Relationships," Whirlpool Project Report, May 15, 1967.
3. Tibbitts, W. I., "Clothes Drying Process," Whirlpool Research Report, June 14, 1960.
4. Hughes, L. H., "Preliminary Investigation of the Falling Rate Region of Convective Drying," Whirlpool Research Report, September 30, 1963.
5. Hughes, L. H., "Convective Dryer Analysis," Whirlpool Research Report, February 12, 1963.
6. Knoop, D. E. and Becker, S., "Design and Analysis of an Electric Range Surface Unit Control System," Whirlpool Project Report, July 29, 1968.
7. Becker, S. and Knoop, D. E., "A Solid State Temperature Control for Electric Range Surface Units," Whirlpool Project Report, July 29, 1968.
8. Melsa, J. L. and Schultz, D. G., Linear Control Systems, McGraw-Hill Book Company, New York, 1969.
9. Rule, W. P., Fortran IV Programming, Prindle, Weber, and Schmidt, Boston, 1968.
10. Roots, W. K. and Walker, F., "Secondary Feedback in ON-OFF Electric Heating Processes," IEEE Transactions on Industry and General Applications, Vol. IGA-3, No. 5, pp. 401-20, September/October, 1967.
11. Roots, W. K. and Walker, F., "Discontinuous Temperature Control," Proceedings of the IEEE, Vol. 112, pp. 511-23, March, 1965.
12. Hanchett, G. D., "Electronic Heat Controls for Appliances and Domestic Heating," IEEE Transactions on Industry and General Applications, pp. 187-92, May/June, 1965.



13. Hsu, J. C. and Meyer, A. V., Modern Control Principles and Applications, McGraw-Hill Book Company, New York, 1968.
14. Horowitz, I. M., Synthesis of Feedback Systems, Academic Press, New York, 1963.
15. De Russo, P. M., Roy, R. J., and Close, C. M., State Variables for Engineers, Wiley, New York, 1967.
16. Sage, A. P., Optimum Systems Control, Prentice Hall, Englewood Cliffs, N. J., 1968.
17. Athans, M., Optimal Control, McGraw Hill Book Company, New York, 1966.